

**AFRL-VA-WP-TR-1999-3069**

**AUTOMATED STRUCTURAL  
OPTIMIZATION SYSTEM (ASTROS)  
DAMAGE TOLERANCE MODULE**

**VOLUME I -- FINAL REPORT**



**L. WANG  
S.N. ATLURI**

**KNOWLEDGE SYSTEMS, INC.  
426 MESA VERDE AVENUE  
PALMDALE, CA 93551**

**FEBRUARY 1999**

**FINAL REPORT FOR 09/30/1996 – 09/30/1998**

**THIS IS A SMALL BUSINESS INNOVATION RESEARCH (SBIR) PHASE II REPORT**

**APPROVED FOR PUBLIC RELEASE; DISTRIBUTION UNLIMITED**

**20000407 064**

**AIR VEHICLES DIRECTORATE  
AIR FORCE RESEARCH LABORATORY  
AIR FORCE MATERIEL COMMAND  
WRIGHT-PATTERSON AIR FORCE BASE OH 45433-7542**

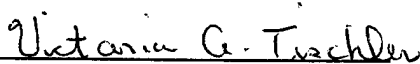
**DTIC QUALITY INSPECTED 1**


## NOTICE

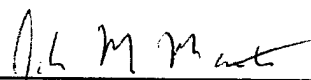
USING GOVERNMENT DRAWINGS, SPECIFICATIONS, OR OTHER DATA INCLUDED IN THIS DOCUMENT FOR ANY PURPOSE OTHER THAN GOVERNMENT PROCUREMENT DOES NOT IN ANY WAY OBLIGATE THE UNITED STATES GOVERNMENT. THE FACT THAT THE GOVERNMENT FORMULATED OR SUPPLIED THE DRAWINGS, SPECIFICATIONS, OR OTHER DATA DOES NOT LICENSE THE HOLDER OR ANY OTHER PERSON OR CORPORATION; OR CONVEY ANY RIGHTS OR PERMISSION TO MANUFACTURE, USE, OR SELL ANY PATENTED INVENTION THAT MAY BE RELATED TO THEM.

THIS REPORT IS RELEASEABLE TO THE NATIONAL TECHNICAL INFORMATION SERVICE (NTIS). AT NTIS, IT WILL BE AVAILABLE TO THE GENERAL PUBLIC, INCLUDING FOREIGN NATIONS.

THIS TECHNICAL REPORT HAS BEEN REVIEWED AND IS APPROVED FOR PUBLICATION.

  
VICTORIA A. TISCHLER  
Aerospace Engineer  
Design and Analysis Branch

  
NELSON D. WOLF, Chief  
Design & Analysis Branch  
Structures Division

  
JOSEPH M. MANTER, Chief  
Structures Division  
Air Vehicles Directorate

IF YOUR ADDRESS HAS CHANGED, IF YOU WISH TO BE REMOVED FROM OUR MAILING LIST, OR IF THE ADDRESSEE IS NO LONGER EMPLOYED BY YOUR ORGANIZATION, PLEASE NOTIFY AFRL/VASD BLDG 146, 2210 8TH STREET, WRIGHT-PATTERSON AFB OH 45433-7531 TO HELP MAINTAIN A CURRENT MAILING LIST.

COPIES OF THIS REPORT SHOULD NOT BE RETURNED UNLESS RETURN IS REQUIRED BY SECURITY CONSIDERATIONS, CONTRACTUAL OBLIGATIONS, OR NOTICE ON A SPECIFIED DOCUMENT.

REPORT DOCUMENTATION PAGE			Form Approved OMB No. 0704-0188	
Public reporting burden for this collection of information is estimated to average 1 hour per response, including the time for reviewing instructions, searching existing data sources, gathering and maintaining the data needed, and completing and reviewing the collection of information. Send comments regarding this burden estimate or any other aspect of this collection of information, including suggestions for reducing this burden, to Washington Headquarters Services, Directorate for Information Operations and Reports, 1215 Jefferson Davis Highway, Suite 1204, Arlington, VA 22202-4302, and to the Office of Management and Budget, Paperwork Reduction Project (0704-0188), Washington, DC 20503.				
1. AGENCY USE ONLY (Leave blank)		2. REPORT DATE FEBRUARY 1999		3. REPORT TYPE AND DATES COVERED FINAL REPORT FOR 09/30/1996 - 09/30/1998
4. TITLE AND SUBTITLE AUTOMATED STRUCTURAL OPTIMIZATION SYSTEM (ASTROS) DAMAGE TOLERANCE MODULE			5. FUNDING NUMBERS C F33615-96-C-3215 PE 65502 PR 3005 TA 41 WU 91	
6. AUTHOR(S) L. WANG S.N. ATLURI				
7. PERFORMING ORGANIZATION NAME(S) AND ADDRESS(ES) KNOWLEDGE SYSTEMS, INC. 426 MESA VERDE AVENUE PALMDALE, CA 93551			8. PERFORMING ORGANIZATION REPORT NUMBER	
9. SPONSORING/MONITORING AGENCY NAME(S) AND ADDRESS(ES) AIR VEHICLES DIRECTORATE AIR FORCE RESEARCH LABORATORY AIR FORCE MATERIEL COMMAND WRIGHT-PATTERSON AFB, OH 45433-7542 POC: VICTORIA A. TISCHLER, AFRL/VASD, 937-255-9729			10. SPONSORING/MONITORING AGENCY REPORT NUMBER  AFRL-VA-WP-TR-1999-3069	
11. SUPPLEMENTARY NOTES  THIS IS A SMALL BUSINESS INNOVATION RESEARCH (SBIR) PHASE II REPORT.				
12a. DISTRIBUTION AVAILABILITY STATEMENT  APPROVED FOR PUBLIC RELEASE, DISTRIBUTION UNLIMITED.			12b. DISTRIBUTION CODE	
13. ABSTRACT (Maximum 200 words) This report was developed under SBIR contract. This report is part of the documentation that describes the complete development of an SBIR Phase II effort titled, "An ASTROS Compatible Computational Strategy for Evaluating the Aeroelastic Response, Buckling, and Integrity of Composite A/C". This report is one of three manuals that comprise the final documentation. The remaining reports consist of a User's Manual, Volume II, and an Interface Design Document, Volume III.  The Automated STRuctural Optimization System (ASTROS) is a multidisciplinary computer program for the preliminary design of aircraft and spacecraft structures. It integrates structures, aerodynamics, controls and optimization to make possible interdisciplinary design.  This report describes the work performed to enhance the capability of ASTROS to perform preliminary design optimization of metallic and composite material aircraft, based on damage tolerance requirements. It defines the SBIR technical objectives and gives a technical description of the Damage Tolerance models. The Automated global-local analyzer, the Buckling analysis of a composite with/without delamination, the Finite Element Alternating Method, Fatigue crack growth and optimization are also discussed. Finally a short description of interfacing with ASTROS is given.				
14. SUBJECT TERMS Damage Tolerance Models, Master Element Approach, Automated Global-local Analyzer, Preliminary Design Optimization, Buckling Analysis, Composites, Delamination, Finite Element Alternating Method, Fatigue Crack Growth			15. NUMBER OF PAGES 62	
			16. PRICE CODE	
17. SECURITY CLASSIFICATION OF REPORT UNCLASSIFIED	18. SECURITY CLASSIFICATION OF THIS PAGE UNCLASSIFIED	19. SECURITY CLASSIFICATION OF ABSTRACT UNCLASSIFIED	20. LIMITATION OF ABSTRACT SAR	

# TABLE OF CONTENTS

<b>LIST OF FIGURES</b>	<b>v</b>
<b>CHAPTER</b>	<b>1</b>
<b>I Introduction</b>	<b>1</b>
1.1 Introduction . . . . .	1
1.2 SBIR Technical Objectives . . . . .	3
<b>II Technical Description</b>	<b>7</b>
2.1 Master-element approach . . . . .	7
2.2 Damage tolerance models . . . . .	8
2.2.1 2D through wall crack . . . . .	8
2.2.2 2D through wall cracks emanating from a hole . . . . .	9
2.2.3 Surface flaw . . . . .	10
2.2.4 Corner cracks emanating from a hole . . . . .	11
2.2.5 2D through wall curved crack . . . . .	11
2.2.6 2D through wall curved cracks emanating from a hole . . . . .	12
2.2.7 Discrete source damage . . . . .	13
2.2.8 BUCKDEL . . . . .	14
2.3 Automated global-local analyzer . . . . .	14
2.3.1 Hierarchical analysis methodology . . . . .	15
2.3.2 Geometry Modeling and Mesh Generation . . . . .	16
2.3.3 Analysis Model and Feature Modeling . . . . .	21
2.3.4 Hierarchical Analysis Based on Feature Modeling . . . . .	22
2.4 Buckling Analysis of a Composite with/without delamination . . . . .	25
2.5 Finite Element Alternating Method . . . . .	29
2.5.1 Superposition Principle and the Alternating Method . . . . .	29
2.5.2 Convergence of the Alternating Method . . . . .	32
2.5.3 Summary of FEAM Procedure . . . . .	34
2.5.4 2D FEAM for straight cracks . . . . .	35
2.5.5 3D FEAM for surface flaws and corner cracks . . . . .	37
2.5.6 Distributed-Dislocation-base FEAM for curved cracks . . . . .	44
2.6 Fatigue crack growth . . . . .	44
2.7 Optimization . . . . .	47
2.8 Interfacing with ASTROS . . . . .	48
2.8.1 MAPOL . . . . .	49
2.8.2 DATABASE . . . . .	49
2.8.3 TCL . . . . .	49

<b>III Summary of Phase II Accomplishments</b>	<b>52</b>
<b>REFERENCES</b>	<b>54</b>

# LIST OF FIGURES

1.1	Central Crack and Broken Stiffener in a Panel	4
1.2	Failed Lower Wing Panel of a U.S. Air Force C-141B Due to the Growth of a Surface Flaw	5
1.3	Hole in the Upper (Compression) Skin of a Wing	5
1.4	Delamination Due to Impact of a Laminated Composite	6
2.1	A through wall crack	9
2.2	Two cracks emanating from a hole	9
2.3	A surface flaw of the shape of semi-ellipse/circle	10
2.4	Two corner cracks emanating from a hole	11
2.5	A curved crack	12
2.6	The curved cracks emanating from a rivet hole	13
2.7	A lead crack in a stiffened panel with/without a broken central stiffener	13
2.8	Buckling of a composite panel with elliptical/circular delamination	14
2.9	A design optimization model	16
2.10	A Global Analysis	17
2.11	The Isolated Skin (Local Model)	17
2.12	Damage in the Upper (Compression) Skin of a Wing	26
2.13	Superposition Principle for Finite Element Alternating Method	30
2.14	Subtract $\lambda P_{FEM}$ from $P_{ANA}$ to Obtain the Solution for $P_{RES}$ which has Homogeneous Boundary Condition on $\Gamma$	33
2.15	Convergence Criterion	35
2.16	Superposition Principle Used in the Finite Element Alternating Method	36
2.17	Flow Chart of the Finite Element Alternating Method	38
2.18	The Finite Element Mesh When a) The EDI Method is Used; b) The Finite Element Alternating Method is Used	39
2.19	U.S. Air Force C-141B	43
2.20	Cut-Out Lower Wing Panel from the C-141B Showing Weep Holes	43
2.21	Cross-Section of Failed Lower Wing Panel of the C-141B	44



# FOREWORD

This is the final report on the work performed by Knowledge Systems, Inc. on the U.S. Air Force Contract F33615-96-C-3215, "An ASTROS Compatible Strategy for Evaluating the Aeroelastic Response, Buckling and Integrity of Composite A/C". This report contains 3 parts: 1) "ASTROS Damage Tolerance Module: Final Report"; 2) "ASTROS Damage Tolerance Module: Interface Design Document"; and 3) "ASTROS Damage Tolerance Module: User's Manual".

This report details the work performed to enhance the capability of ASTROS to perform preliminary design optimization of metallic and composite material aircraft, based on damage tolerance requirements. The customized damage tolerance models that have been implemented in ASTROS, at present, are:

1. Discrete Source Damage Model: A lead crack in a stiffened panel with/without the presence of a central broken stiffener;
2. BuckDel model: Buckling of a composite panel in the presence of a delamination;
3. Straight Crack Model: A panel with a central crack;
4. Rivet Hole Crack Model: One (or two) crack(s) emanating from one side (or both sides) of a rivet hole;
5. Curved Crack Model: A panel with a curved crack;
6. Rivet Hole Curved Crack Model: One (or two) curved crack(s) emanating from one side (or both sides) of a rivet hole;
7. Surface Crack Model: One centered surface crack in a plate;
8. Rivet Hole Corner Crack Model: Two corner cracks emanating from both the sides of a straight-shank rivet hole.

The authors acknowledge the contributions of D.S. Pipkins, P.E. O'Donoghue, K. O'Sullivan, and H. Kawai to various parts of this report.

It is a pleasure to acknowledge the constant support, constructive criticism, and valuable insights, provided by Drs. V.A. Tischler and V.B. Venkayya of AFRL during the course of this project.



# CHAPTER I

## INTRODUCTION

### 1.1 Introduction

In addition to requirements such as strength, stiffness, and aeroelastic response it is necessary to design both metallic and composite aircraft structures to withstand the effects of damage. By doing so, safe, economical fleets with high operational readiness can be insured. The importance of safety and operational readiness to profitability and competitiveness in a commercial aviation setting and national defense in a military one is apparent. To insure that metallic aircraft structures are designed and maintained to withstand the effects of damage, the Federal Aviation Administration (FAA) and United States Air Force (USAF) have established specific guidelines which must be followed. The FAA requires commercial transport aircraft certified under part 25 of the Federal Aviation Regulations (FAR) to meet certain Damage Tolerance Requirements (DTR). Similarly, the USAF has specified a set of DTR for metallic structures which are described in detail in MIL-STD-1530A. For composite structures, the FAA does not have formal requirements for certification at this time. The Air Force, on the other hand, has specified a set of DTR for composite structures in AFGS-87221A. The DTR, as set forth by both the FAA and the Air Force, essentially state that:

- the residual strength of an airframe structural component shall not drop below that required to sustain limit load, and
- that inspections must be scheduled to insure that the required level of residual strength is maintained.

The primary means by which the DTR are satisfied by commercial and military airframe manufacturers and maintenance organizations is through the performance of a Damage Tolerance Assessment (DTA). The DTA involves the development of damage growth curves and residual strength diagrams for individual structural components of an airframe. This allows the residual strength as a function of aircraft usage to be determined. With this information, manufacturers can design components which minimize the evolution and growth of damage and its effect on the integrity of the aircraft structure. Further, appropriate inspection intervals can be specified which insure that the structural integrity of the aircraft will be maintained through out its life.

At present, there is no other software which integrates damage tolerance with the other disciplines (i.e. strength, stiffness, aeroelastic response, etc.) which impact the design of an aircraft structure. As a result, the design of an aircraft structure which satisfies damage tolerance requirements in addition to those of other disciplines, is presently accomplished via a manual "cut and try" procedure. This type of design process is time consuming and therefore very costly [Nees

(1995)]. To address this deficiency in existing software, this SBIR project is implementing a damage tolerance module into the multidisciplinary analysis and design software, ASTROS.

Phase I of this SBIR project has addressed the damage tolerance analysis of aircraft structures made of laminated composites. The damage considered was in the form of a delamination between lamina in a stiffened panel. The Phase I effort accomplished the following.

- Damage tolerance software applicable to laminated composites, called BUCKDEL, was developed. The BUCKDEL software performs a geometrically nonlinear analysis of stiffened laminated composite plates with and without delaminations. BUCKDEL allows the user to perform: a linear static solution; a linear buckling (eigenvalue) analysis; and a nonlinear post-buckling analysis through both limit and bifurcation points. BUCKDEL also calculates the pointwise energy release rates around a delamination front using an Equivalent Domain Integral (EDI) technique. The energy release rates can be used to predict the growth and onset of unstable propagation of a delamination.
- The feasibility of using a global-local approach to link an ASTROS finite element analysis (global) with a local damage analysis (such as that performed by BUCKDEL) was investigated. This global-local approach was found to be workable, due in large part to the ASTROS system architecture which allows the user to introduce special purpose modules by making use of the SYSGEN program which is provided with ASTROS.

Based on the Phase I results, the implementation of a damage tolerance module into ASTROS which accounts for typical damage in both composite and metallic structure is feasible. This report describes the Phase II effort in the implementation of the damage tolerance module in ASTROS. In addition to this report, the users' manual and the interface design document for the damage tolerance module are prepared as part of the documentation for this project.

In phase II of this SBIR project, customized Damage Tolerance Models (DT model) are implemented in ASTROS. Customized damage tolerance models are idealized damage scenarios that are to be considered for damage tolerance requirements. Localized damage, such as a crack or delamination, is very small in size when compared to the finite element model used in preliminary design optimization. Therefore, these damages are not modeled explicitly in the FEM model for preliminary design optimization. The damage tolerance module automatically generates detailed computational models for damage tolerance assessment, using a few parameters for the definition of the DT models via bulk data cards introduced by the damage tolerance module. This feature of the damage tolerance module greatly simplifies the model preparation effort for the user in the preliminary design phase. The customized DT models that have been implemented in ASTROS at present are:

- Discrete Source Damage Model: a lead crack in a stiffened panel with/without the presence of a broken central stiffener [Fig. 2.7]
- BuckDel Model: buckling of a composite panel in the presence of a delamination [Fig. 2.8]
- Straight Crack Model: a panel with a centered crack [Fig. 2.1]

- Rivet Hole Crack model: one (or two) crack(s) emanating from one side (or both sides) of a rivet hole [Fig. 2.2]
- Curved Crack model: a panel with a curved crack [Fig. 2.5]
- Rivet Hole Curved Crack model: one (or two) curved crack(s) emanating from one side (or both sides) of a rivet hole [Fig. 2.6]
- Surface crack model: one centered surface crack in a plate [Fig. 2.3]
- Rivet Hole Corner Crack model: two corner cracks emanating from both side of a straight-shank rivet hole. [Fig. 2.4]

A master element approach has been implemented in ASTROS to access these damage tolerance models. Using these models the user can evaluate fracture parameters or perform fatigue crack growth analyses. Damage tolerance based constraints for the design optimization can then be used in the preliminary design optimization.

## 1.2 SBIR Technical Objectives

The objective of this SBIR project is to develop damage tolerance software as an analysis module in the multidisciplinary analysis and design software, ASTROS. The software uses state of the art, computationally efficient algorithms for determining the residual strength and life [Atluri (1995)] of metallic and composite structures with damage. It enhances the existing capabilities of ASTROS by allowing constraints based on damage tolerance requirements to be considered simultaneously with those based on strength, stiffness, aeroelastic response, etc. during design optimization. Included in potential commercial applications of such a capability are industries involved in the design of aircraft structures, automobiles, bridges and buildings.

ASTROS is well suited for modeling the global strength, stiffness, and aeroelastic response of an undamaged, stiffened structure. However, it presently does not have the capability to account for local damage such as cracks, delaminations, and penetration holes. Therefore, this SBIR project is to develop a damage tolerance module for ASTROS. The damage tolerance module

- utilizes the existing capabilities of ASTROS for performing the modeling of the structure;
- generates load spectra in terms of ASTROS load cases;
- develops customized damage tolerance modules to model local damages in metallic and composite materials;
- has a seamless interface to the other modules in ASTROS, via an engineering database and high level programming language (MAPOL).
- defines new bulk data entries, relational schema and error messages needed to provide a consistent interface as the other modules in ASTROS.

The damage scenarios considered in the damage tolerance module are:

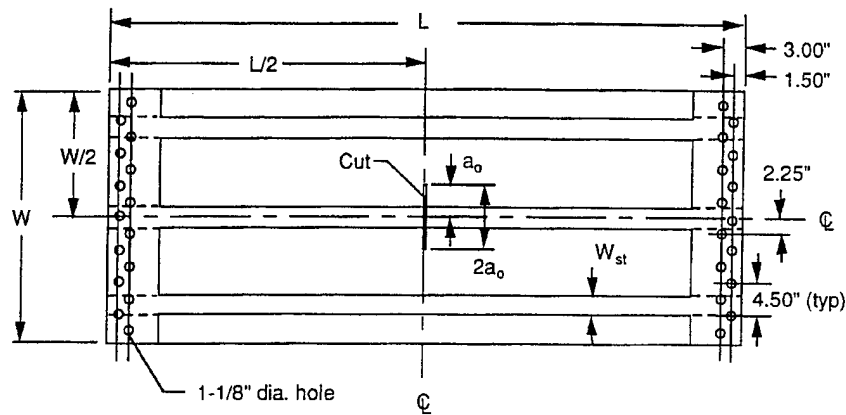


Figure 1.1: Central Crack and Broken Stiffener in a Panel

- single or multiple skin cracks (Widespread Fatigue Damage) in a stiffened structure, including the effect of broken stiffeners (Fig. 1.1) [tensile loading, metallic and composite materials];
- skin crack turning at stiffeners [tensile loading, metallic and composite materials];
- single or multiple part elliptical/circular surface flaws at holes or other stress raisers (Fig. 1.2) [tensile loading; metallic materials]
- holes (Fig. 1.3) [compressive loading, metallic and composite materials]; and
- delaminations (Fig. 1.4)[compressive loading, composite materials].

For metallic or composite aircraft structures loaded in tension, the damage of principal interest during design is usually in the form of cracks normal to the direction of principal tension. These cracks typically occur over time due to fatigue or suddenly due to an event such as an uncontained failure of a rotating engine component or battle damage. A crack arising suddenly due to a catastrophic event is an example of discrete source damage (DSD). In reality, DSD in a structure loaded in tension such as a fuselage or lower wing would be in the form of an irregular shaped hole. However, since a crack of length ' $a$ ' is more critical than a hole of diameter ' $a$ ', the crack representation of DSD represents a worst case scenario. Therefore, for reasons of conservatism and practicality (both experimental and analytical) the crack is used in the certification of primary structural elements loaded in tension. Residual strength and life calculations for structures containing cracks and loaded in tension will be based on Linear Elastic Fracture Mechanics (LEFM). Thus, the parts of the damage tolerance modules which analyze cracked structure will compute stress intensity factors and their sensitivities to changes in the design variables. These values can then be used to evaluate constraints based on residual strength requirements. For constraints based on residual life (fatigue) requirements, the computed stress intensity factors will be used in crack growth equations to determine the time required for a crack or cracks to grow to a critical size. The

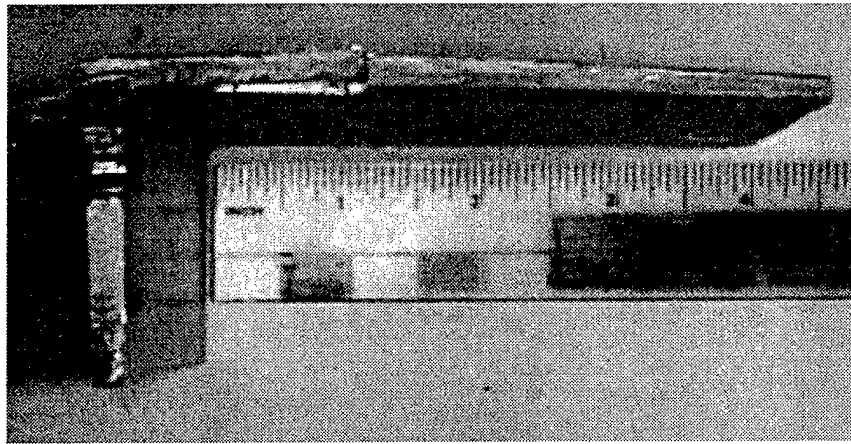


Figure 1.2: Failed Lower Wing Panel of a U.S. Air Force C-141B Due to the Growth of a Surface Flaw

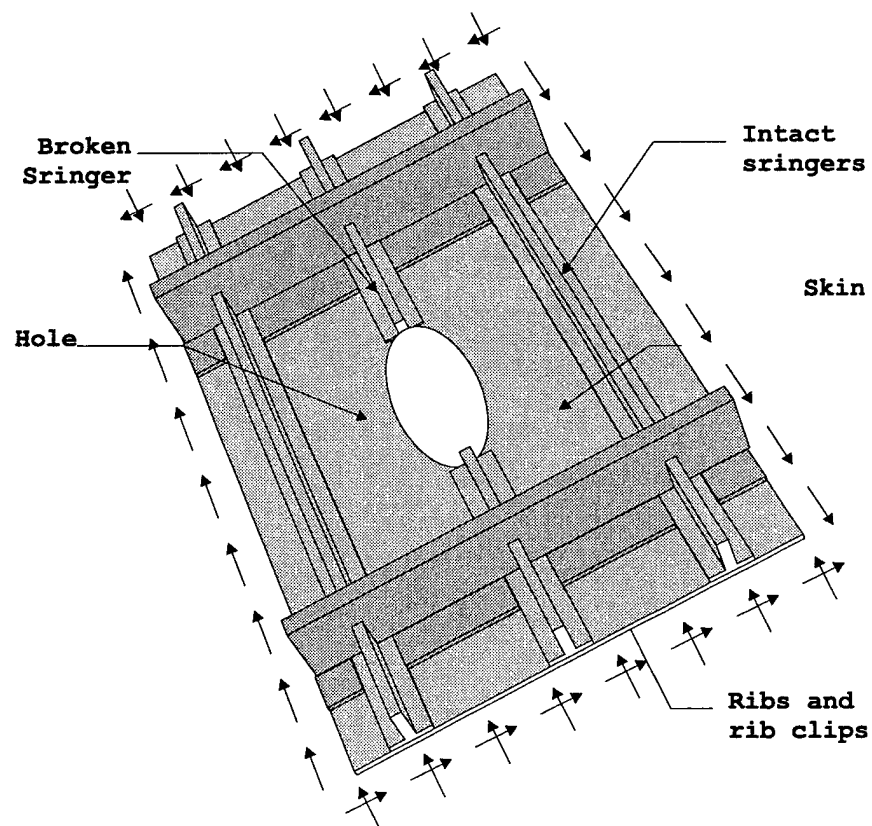


Figure 1.3: Hole in the Upper (Compression) Skin of a Wing

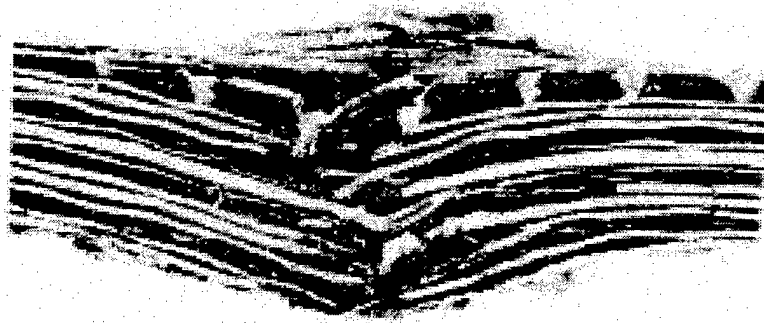


Figure 1.4: Delamination Due to Impact of a Laminated Composite

critical size is determined from a residual strength requirement such as that requiring the structure to be able to sustain limit load at any time in its life.

For metallic or composite aircraft structures loaded in compression, the primary concern is with DSD in the form of a hole or crack parallel to the direction of principal compression. For laminated composites, delaminations between lamina are also of concern. Delaminations can result from excessive interlaminar shear stresses or through-the-thickness tensile stresses at holes, free edges, section changes, or in bonded joints; panel buckling; and low velocity impact. The modeling of delaminations in laminated composites was addressed in Phase I and resulted in the development of the BUCKDEL software. The residual strength of structures loaded in compression will be based on the buckling and post-buckling behavior of the structure. For laminated composites containing delaminations, the pointwise energy release rate around the delamination front will also be used in the residual strength prediction.

The motivation for modeling DSD in a structure loaded in compression in the form of a hole or crack parallel to the direction of principal compression is as follows. For a stiffened structure, the buckling load is expected to vary significantly with the size, shape (i.e. circular or elliptical), and location (i.e. distance from the wing tip) of the hole. Some results reported in the literature [Vellaichamy et. al (1990), Nemeth (1990), and Britt (1994)] indicate, as is to be expected, that for an elliptical hole with the major axis along the direction of compression, the initial buckling load is lower than that for a circular hole of the same area. Similarly, if a panel is subject to pure shear in the  $x$ - $y$  plane, the shear buckling load will be minimum when the major axis of the ellipse is at 45 degrees to the  $x$  axis. The buckling load will decrease with an increase in the aspect ratio of the ellipse. The most severe case being in the limit when the ellipse degenerates into a crack (with the crack axis along the direction parallel to the direction of compression). Based upon this discussion, it is anticipated that the worst case DSD scenario for primary structure loaded in compression will be a crack oriented such that its axis is parallel to the direction of maximum compressive stress.

## **CHAPTER II**

### **TECHNICAL DESCRIPTION**

This chapter describes the technical details in the damage tolerance module in ASTROS. The damage tolerance module in ASTROS uses a master-element approach to extract loading conditions for the damage tolerance models. An automated global-local analyzer is used to perform hierarchical analysis of discrete source damage. An integrated geometry modeler and mesh generator is used to construct damage tolerance models using a few user specified parameters. Finite element alternating methods are used for the evaluations of stress intensity factors for straight or curved cracks, 3D cracks of elliptical/circular shape. BUCKDEL is used for the evaluation of the buckling load of a composite panel with delamination. A load spectrum module is used to generate fatigue loading history in terms of ASTROS loading cases. Details of these techniques are described in this chapter. The reader is assumed to be familiar with ASTROS (Automated STRuctural Optimization System).

#### **2.1 Master-element approach**

A master-element approach is used to enable the automatic generation of loading conditions for damage tolerance models. Localized damages, such as a crack or delamination, are very small in size when compared to the overall finite element model used in the preliminary design optimization. Therefore, these damages are not modeled explicitly using FEM mesh during the preliminary design optimization. For each of the damages specified in the preliminary design model, a separate damage tolerance model is generated for damage tolerance assessment.

A master element is the element in the Preliminary Design model (PD model) that contains the damage under consideration. Since it is small in size, the damage's effect on the load flow in the PD model is practically negligible. Therefore, the loading condition in the master element of the PD model (without damage) represents the loading condition for the panel with a damage. Based on this assumption the damage tolerance module extracts the loading information from the master element from the engineering database after the static mechanical analysis, and generates the Damage Tolerance model (DT model) for damage tolerance assessment.

The damage tolerance module automatically generates detailed computational models for damage tolerance assessment, using a few parameters for the definition of the DT models via bulk data cards introduced by the damage tolerance module. This feature of the damage tolerance module greatly simplifies the model preparation effort for the user in the preliminary design phase.

There are a number of advantages in using the master-element approach. The master-element approach, together with the high level of abstraction of the damage tolerance model, makes it

possible for the development of interchangeable modules for performing the damage tolerance assessment for the same damage using different methods.

The master-element approach allows the damage tolerance module to treat different types of damage in a similar fashion.

When the master-element approach is used, the damage tolerance analysis imposes no additional requirements on the preparation of the PD model. A single PD model can be used to assess multiple damage scenarios with a single or multiple damage.

However, the master-element approach can not be used when the size of a damage is so large that the loading conditions around the damage are altered significantly due to its presence. This may occur in the analyses of the structural details where the size of the damage is not small when compared to the structural details in the FEM under consideration. In such a case the effect of the damage on the load distribution must be taken into account in order to assess the capacity of the damage tolerance of the structure.

## 2.2 Damage tolerance models

Although the structural details in the vicinity of a crack have significant influence on the stress intensity factors of the crack, such details are to be determined in the later stage of design. Therefore, accurate modeling of structural details in the vicinity of a crack for specific location is not necessary in the phase of preliminary design. However, it is necessary to model the “average” structural behaviors so that the overall damage tolerance capability of the structure can be achieved in preliminary design, where the interaction between multiple disciplines requires intensive computation. Once the preliminary design ensures that the structure has adequate *overall* damage tolerance capability, the detailed design (which does not involve multiple disciplines) can easily meet the damage tolerance requirement by changing the structural details near the critical locations.

This section describes the customized damage tolerance models that have been implemented into ASTROS.

### 2.2.1 2D through wall crack

In this damage model [see Fig. 2.1], a small crack is located at the center of a panel. When the dimension of the panel is not explicitly specified by the user, the damage tolerance module will calculate the dimension based on the size of the master element. A square panel will be generated with an area equal to that of the master element. A coordinate transformation is performed by the damage tolerance module so that the crack is on the  $x$ -axis in the damage tolerance model as seen in Fig. 2.1. The loading condition is taken from the corresponding master element. A 2D plane stress analysis is performed. The beta factors for mode I and mode II SIFs are defined as:

$$\beta_1 = \frac{K_I}{\sigma_y \sqrt{\pi a}}, \quad \beta_2 = \frac{K_{II}}{\sigma_{xy} \sqrt{\pi a}}$$

where  $\sigma_y$  and  $\sigma_{xy}$  are the normal and shear stresses in the master element in the crack coordinate system.



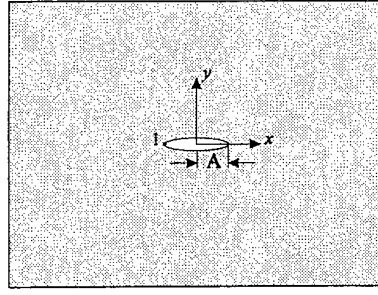


Figure 2.1: A through wall crack

The user can choose from one of the following methods to perform the fracture analysis. They are i) 2D finite element alternating method (FEAM); ii) using user supplied beta factors; iii) using infinite body solution. In practice, one can use the 2D FEAM to calculate the beta factor; then, use the beta factor in the subsequent analyses.

### 2.2.2 2D through wall cracks emanating from a hole

In this damage model [see Fig. 2.2], one (or two) small crack(s) emanates from a rivet hole at the center of a panel. When the dimension of the panel is not explicitly specified by the user, the damage tolerance module will calculate the dimension based on the size of the master element. A square panel will be generated with an area equal to that of the master element. A coordinate transformation is performed by the damage tolerance module so that the cracks are on the x-axis in the damage tolerance model as seen in Fig. 2.2. The loading condition is taken from the corresponding master element. A 2D plane stress analysis is performed. The beta factors for mode I and mode II SIFs are defined as:

$$\beta_1 = \frac{K_I}{\sigma_y \sqrt{\pi a}}, \quad \beta_2 = \frac{K_{II}}{\sigma_{xy} \sqrt{\pi a}}$$

where  $\sigma_y$  and  $\sigma_{xy}$  are the normal and shear stresses in the master element in the crack coordinate system;  $a = r + (a_1 + a_2)/2$ .

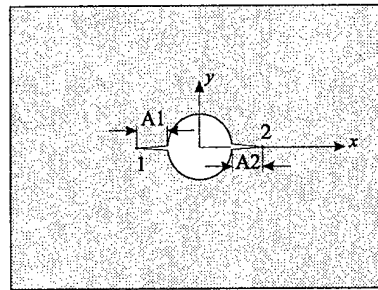


Figure 2.2: Two cracks emanating from a hole

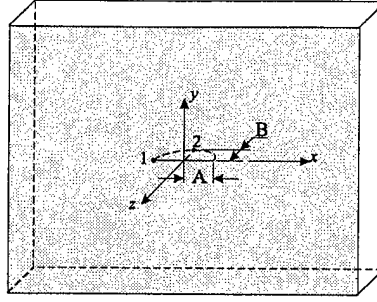


Figure 2.3: A surface flaw of the shape of semi-ellipse/circle

When there are two cracks emanating from the hole, these two cracks must be aligned in a line passing through the center of the hole.

The user can choose from one of the following methods to perform the fracture analysis. They are i) 2D finite element alternating method (FEAM); ii) using user supplied beta factors; iii) using infinite body solution. In practice, one can use the 2D FEAM to calculate the beta factor; then, use the beta factor in the subsequent analyses.

### 2.2.3 Surface flaw

In this damage model [see Fig. 2.3], a surface flaw is located at the center of a panel. The surface flaw is of a half elliptical/circular shape. The major (or the minor) axis aligns with the surface; while the other axis is in the thickness direction. When the length and width of the panel are not explicitly specified by the user, the damage tolerance module will calculate the dimensions based on the size of the master element. A square panel will be generated with area equal to that of the master element. If the user does not specify the thickness explicitly, the thickness of the master element is used. A coordinate transformation is performed by the damage tolerance module so that the surface flaw is in the  $x$ - $z$  plane in the damage tolerance model as seen in Fig. 2.3. The loading condition is taken from the corresponding master element. The beta factors for mode I, mode II, and mode III SIFs are defined as:

$$\beta_1 = \frac{K_I}{\sigma_y \sqrt{\pi \bar{a}}}, \quad \beta_2 = \frac{K_{II}}{\sigma_{xy} \sqrt{\pi \bar{a}}}, \quad \beta_3 = \frac{K_{III}}{\sigma_{xy} \sqrt{\pi \bar{a}}}$$

where  $\sigma_y$  and  $\sigma_{xy}$  are the normal and shear stresses in the master element in the crack coordinate system;  $\bar{a} = \min(a, b)$ .

The user can choose from one of the following methods to perform the fracture analysis. They are i) 3D finite element alternating method (FEAM); ii) using user supplied beta factors. In practice, one can use the 3D FEAM to calculate the beta factor; then, use the beta factor in the subsequent analyses.

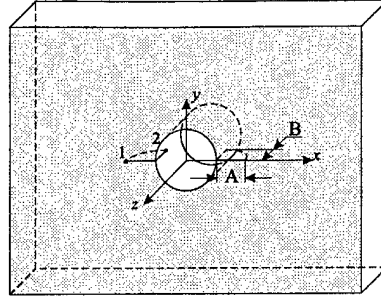


Figure 2.4: Two corner cracks emanating from a hole

#### 2.2.4 Corner cracks emanating from a hole

In this damage model [see Fig. 2.4], two corner cracks symmetrically emanate from a hole at the center of a panel. The two corner cracks have the same size. They are of a quarter elliptical/circular shape. The major (or the minor) axis aligns with the surface; while the other axis is in the thickness direction along the surface of the hole. When the length and width of the panel are not explicitly specified by the user, the damage tolerance module will calculate the dimension based on the size of the master element. A square panel will be generated with an area equal to that of the master element. If the user does not specify the thickness explicitly, the thickness of the master element is used. A coordinate transformation is performed by the damage tolerance module so that the surface flaw is in the  $x$ - $z$  plane in the damage tolerance model as seen in Fig. 2.4. The loading condition is taken from the corresponding master element. The beta factors for mode I, mode II, and mode III SIFs are defined as:

$$\beta_1 = \frac{K_I}{\sigma_y \sqrt{\pi a}}, \quad \beta_2 = \frac{K_{II}}{\sigma_{xy} \sqrt{\pi a}}, \quad \beta_3 = \frac{K_{III}}{\sigma_{xy} \sqrt{\pi a}}$$

where  $\sigma_y$  and  $\sigma_{xy}$  are the normal and shear stresses in the master element in the crack coordinate system;  $\bar{a} = \min(a, b)$ .

The user can choose from one of the following methods to perform the fracture analysis. They are i) 3D finite element alternating method (FEAM); ii) using user supplied beta factors. In practice, one can use the 3D FEAM to calculate the beta factor; then, use the beta factor in the subsequent analyses.

#### 2.2.5 2D through wall curved crack

In this damage model [see Fig. 2.5], a curved crack is located in a panel. The crack is defined piecewise-linearly by a number of points on the crack. When the dimension of the panel is not explicitly specified by the user, the damage tolerance module will calculate the dimension based on the size of the master element. A square panel will be generated with an area equal to that of the master element. The loading condition is taken from the corresponding master element. A 2D

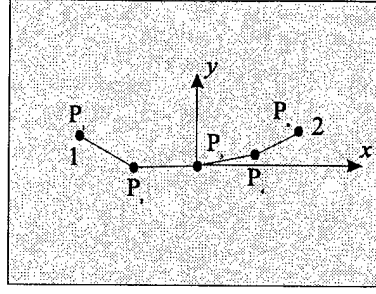


Figure 2.5: A curved crack

plane stress analysis is performed. The beta factors for mode I and mode II SIFs are defined as:

$$\beta_1 = \frac{K_I}{\sigma_y \sqrt{\pi a}}, \quad \beta_2 = \frac{K_{II}}{\sigma_{xy} \sqrt{\pi a}}$$

where  $\sigma_y$  and  $\sigma_{xy}$  are the normal and shear stresses in the master element in the coordinate system for the equivalent crack. The equivalent crack is defined by the straight line connecting the two crack tips of the curved crack.  $a$  is the half length of the equivalent crack.

The user can choose from one of the following methods to perform the fracture analysis. They are i) 2D distributed-dislocation-based finite element alternating method (DFEAM); ii) using user supplied beta factors. In practice, one can use the 2D DFEAM to calculate the beta factor; then, use the beta factor in the subsequent analyses.

### 2.2.6 2D through wall curved cracks emanating from a hole

In this damage model [see Fig. 2.6], one (or two) curved crack(s) emanates from a hole at the center of a panel. The crack is defined piecewise-linearly by a number of points on the crack. When the dimension of the panel is not explicitly specified by the user, the damage tolerance module will calculate the dimension based on the size of the master element. A square panel will be generated with an area equal to that of the master element. The loading condition is taken from the corresponding master element. A 2D plane stress analysis is performed. The beta factors for mode I and mode II SIFs are defined as:

$$\beta_1 = \frac{K_I}{\sigma_y \sqrt{\pi a}}, \quad \beta_2 = \frac{K_{II}}{\sigma_{xy} \sqrt{\pi a}}$$

where  $\sigma_y$  and  $\sigma_{xy}$  are the normal and shear stresses in the master element in the coordinate system for the equivalent crack. The equivalent crack is defined by the straight line connecting the two crack tips of the curved crack.  $a$  is the half length of the equivalent crack.

The user can choose from one of the following methods to perform the fracture analysis. They are i) 2D distributed-dislocation-based finite element alternating method (DFEAM); ii) using user supplied beta factors. In practice, one can use the 2D DFEAM to calculate the beta factor; then, use the beta factor in the subsequent analyses.

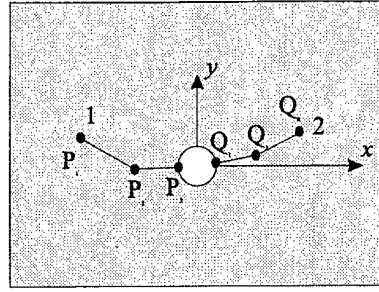


Figure 2.6: The curved cracks emanating from a rivet hole

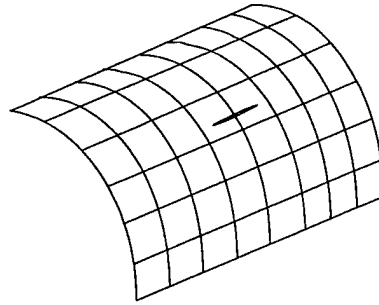


Figure 2.7: A lead crack in a stiffened panel with/without a broken central stiffener

### 2.2.7 Discrete source damage

In this damage model [see Fig. 2.7], one crack is located at the center of a stiffened panel. It can be a pressurized curved panel or a flat panel. The crack is either parallel to the frame or to the stringer. The user can specify whether the center stiffener, passing across the crack, is broken or not. The user must specify the panel size so that a global damage tolerance model can be analyzed to capture the load flow in the panel due to the crack. The loading condition for the global damage tolerance model is obtained from the master element. The automatic global-local analyzer extracts a local model with boundary conditions obtained from the analysis of the global damage tolerance model. A local analysis based on FEAM is performed to obtain the stress intensity factors. The beta factors for mode I and mode II SIFs are defined as:

$$\beta_1 = \frac{K_I}{\sigma_y \sqrt{\pi a}}, \quad \beta_2 = \frac{K_{II}}{\sigma_{xy} \sqrt{\pi a}}$$

where  $\sigma_y$  and  $\sigma_{xy}$  are the normal and shear stresses in the master element in the crack coordinate system.

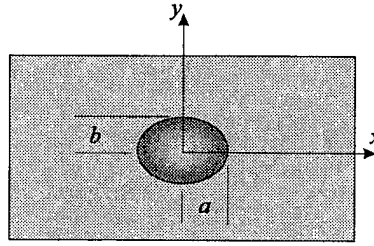


Figure 2.8: Buckling of a composite panel with elliptical/circular delamination

### 2.2.8 BUCKDEL

In this damage model [see Fig. 2.8], an elliptical/circular delamination is located at the center of a panel. When the dimension of the panel is not explicitly specified by the user, the damage tolerance module will calculate the dimensions based on the size of the master element. A square panel will be generated with an area equal to that of the master element. A coordinate transformation is performed by the damage tolerance module so that the major axis of the delamination is in the  $x$ -axis direction as seen in Fig. 2.8. The loading condition is taken from the corresponding master element. The buckling load of the panel is computed using the BUCKDEL module.

## 2.3 Automated global-local analyzer

The damage tolerance analysis of discrete source damage in aging aircraft poses many significant technological challenges. As fracture mechanics treats essentially local phenomena, very detailed modeling of aircraft structures is necessary to analyze discrete source damage. Not only local features (such as fasteners), but also global features (such as stiffeners and joint configurations) must be considered. The fact that an aircraft structure at the global level is a built-up structure assembled from a large number of parts complicates the analysis.

The traditional approach to this problem is to utilize a very large number of elements for embedded local details with aggressive mesh refinement in a coarser global model. The problem is then solved in a single analysis. This approach takes many hours of a very powerful computer to calculate reasonably accurate results using a modern workstation even in the case of a single linear elastic analysis. A parametric survey or design optimization can only be achieved with a supercomputer. In addition, it is very tedious and time consuming to create a finite element mesh with these global and local features in a single model. This makes parametric study and design optimization, which require drastic modification of the mesh, virtually impossible.

Generally, a multi-stage hierarchical approach is a more efficient method for such analyses. However, the inherent complexity of hierarchical analysis and the absence of conventional pre- and post-processors which directly support hierarchical analyses, made this approach impractical until recently. There are several inherent complexities in hierarchical analysis. The first is the simplification of the structure at each coarse stage. The second is the extraction of a subregion

for each detailed analysis. The third is the transfer of boundary conditions, i.e., the conversion from the analysis result in the previous coarse stage to the boundary of the subregion in the next detailed stage. It is obvious that sophisticated support of pre- and post-processing is necessary to circumvent these difficulties.

The automated global-local analyzer is based on feature modeling technology, which has been recently adopted in the field of CAD. Rather than dealing with a finite element model directly at each stage, it deals with a feature model – a high level geometry model. After the feature model and associated analysis conditions are defined, an arbitrary number of stages of hierarchical analyses (including simplification, subregion extraction and boundary condition transfer) can be performed fully automatically. Because the feature model is parametric and defined by several key design parameters, a parametric study can be performed by simply changing the values of these design parameters.

### **2.3.1 Hierarchical analysis methodology**

An automated global-local analysis methodology is used for the analysis of a stiffened structure with discrete source damage.<sup>1</sup> Since the size of the discrete source damage is usually in the same scale as a stiffened panel, it is necessary to model the stiffeners as well as the skin in the damage tolerance model. To reduce computational cost a global-local analysis methodology is used. In the global model cracks are modeled via unconnected nodes at the crack locations. This crude representation of the crack in the global model reflects the loss of stiffness in the structure, so that the redistribution of loads among the skin, stringers and ribs can be captured. Broken stringers and ribs, if any, are also accounted for in a similar manner. The details of the crack tip fields are ignored at this level of analysis. The global analysis results are used to construct a free-body diagram (Fig. 2.11) of the cracked sheet (local model), with the applied loading on the sheet being the reaction forces from stringers and ribs as well as the loading on the periphery of the sheet. The local model is analyzed by the damage tolerance module using a finite element alternating method; while the global model is analyzed by the existing ASTROS module for static analysis.

To illustrate this methodology, consider the case of a wing containing a crack in the skin of the lower surface [Fig. 2.9]. (Note that the methodology is general in nature and can be used for a structure containing damage in the form of penetration holes and/or delaminations.) A coarse finite element mesh is first used to model the global behavior of the cracked panel [Fig. 2.10]. The boundary condition for the global DT model is obtained from the master element in the design model using the master element approach discussed in § 2.1. The traction and/or displacement boundary conditions to be applied to the local model are determined from the results of the global analysis. These boundary conditions include the reaction forces, exerted by the stringers and ribs, on the skin. The Finite Element Alternating Method (FEAM) is used in the local analysis to determine the stress intensity factors. The FEAM allows a coarse finite element mesh to be used

---

<sup>1</sup> Here the global and local model refer to the damage tolerance model generated by the damage tolerance module, as oppose to the preliminary design model used in the process of design optimization.

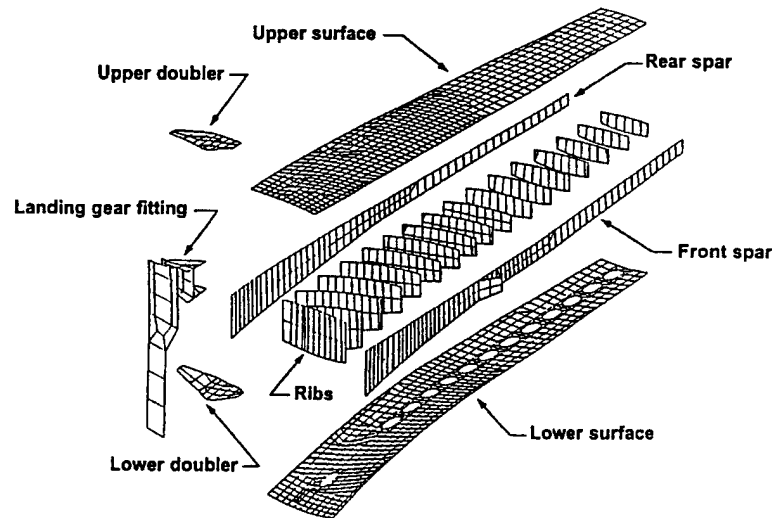


Figure 2.9: A design optimization model

for the local model of the skin because the crack tip fields are captured by an analytical solution and thus cracks need not be modeled explicitly in the mesh. The FEAM along with the other local damage modeling methodologies to be implemented in the damage tolerance module will be discussed in detail in later sections.

Damage in the form of delaminations typically need not be accounted for in the global model. On the other hand, damage in the form of cracks or penetration holes does need to be accounted for if it is of sufficient size to affect the load transfer in the structure.

In the global analysis, the stringers are modeled as beams (ASTROS CBAR elements) attached to the skin (ASTROS CQUAD4), and ribs are modeled as plates (ASTROS CQUAD4). To account for fastener flexibility, beam elements are used to model rivet connections between stiffening elements and the skin. The global model is automatically generated by the integrated geometry modeler and mesh generator in the damage tolerance module. Most details about the automated global-local analyzer are presented in the rest of this section.

### 2.3.2 Geometry Modeling and Mesh Generation

This section describes the most important ingredient of the automatic global-local analyzer: the integrated **GE**ometry modeler and **MESH** generator (GEOMESH). GEOMESH generates the global damage tolerance model, using the user specified geometry parameters for the discrete source damage and the loading condition in the corresponding master element from the preliminary design model. It invokes a separate ASTROS process to perform the global analysis. After the global analysis, it 1) imports the global analysis results; 2) determines the area for local analysis; 3) extracts a detailed boundary condition for the local model (see the free body loading diagram in Fig. 2.11). A summary of how GEOMESH works follows.



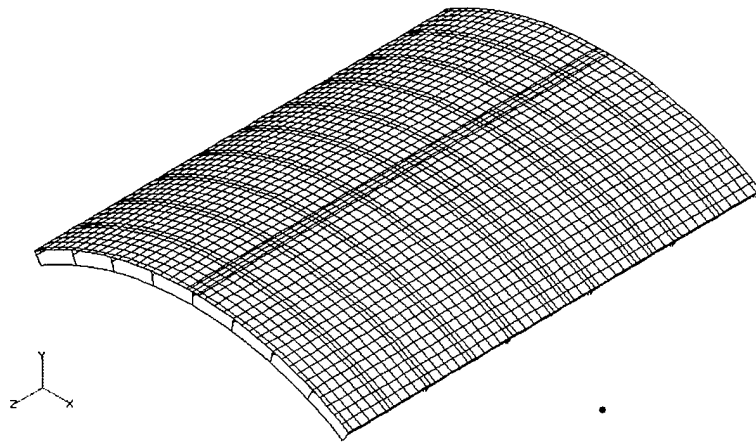


Figure 2.10: A Global Analysis

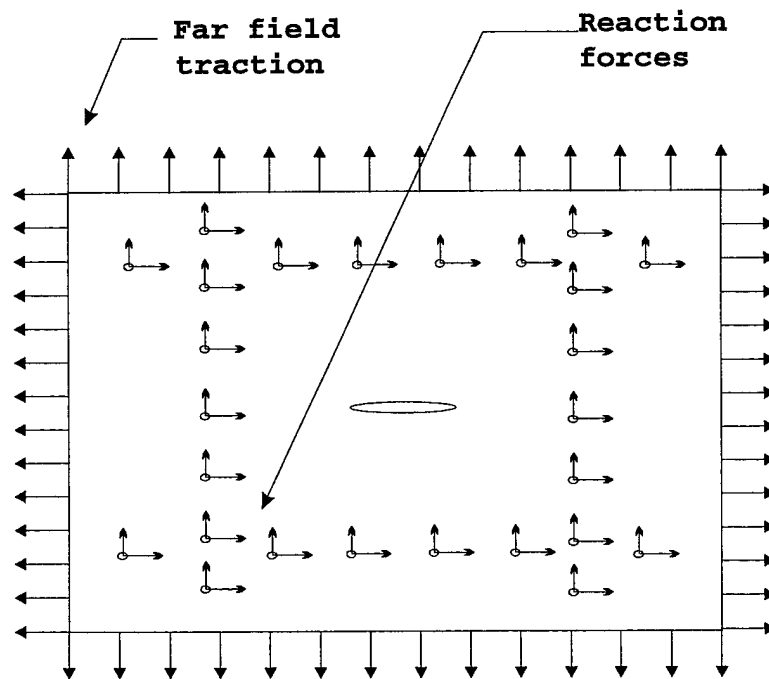


Figure 2.11: The Isolated Skin (Local Model)

1. For each analysis, GEOMESH generates a detailed CAD model representing the entire structure according to the user supplied design parameters.
2. GEOMESH then converts the CAD model into a simplified version of the CAD model. The simplified CAD model has the appropriate level of detail for the current analysis. When an intermediate analysis is necessary, it can also convert global analysis results to the boundary conditions for the intermediate stage. CAD models contain not only geometry information but also the information required for the finite element analysis. These parameters (such as material properties, structural dimensions, body forces and boundary conditions) are associated with geometric entities such as vertices, edges and faces.
3. Finally, a mesh and the associated boundary conditions are generated from the simplified version of the CAD model.

To obtain boundary conditions for the local (or intermediate if necessary) analysis from results of the global analysis, GEOMESH utilizes its post-processing functionalities that extract analysis results at any location in the CAD model. Displacements or stresses can be obtained at any point in the model using a finite element interpolation scheme.

### *Geometry-Based Analysis*

Geometry-based analysis is a relatively new concept in the finite element analysis field. It allows a user to interact with a geometry model to perform analysis rather than to manipulate a mesh directly. This is a mesh-invisible approach wherein the mesh is hidden from the user. A geometry model is defined by a few geometrical parameters. Associated analysis conditions, such as material properties and boundary conditions, are attached to the geometry model. The analysis result can be evaluated at an arbitrary location or region of the geometry model, independent of the elements and the nodes that are hidden behind the geometry model.

A typical geometry model in an engineering field, especially the aircraft industry, can be defined using a small number of dimensional and topological parameters. Once the geometry is parameterized, parametric study can be easily performed.

At first glance, geometry-based analysis seems to have nothing to do with hierarchical analysis. However, subregion definition and simplification are highly problem-dependent in a typical hierarchical analysis. They change frequently or even dynamically in run time during a parametric study. If the user has to directly create and manipulate a finite element model, the mesh generation and boundary condition transfer becomes extremely complex and time consuming. For this reason, hierarchical analysis based on traditional pre- and post-processors, which require the user to manipulate the mesh directly, is largely impractical for parametric study or design optimization. Geometry-based analysis makes this approach practical.

Automatic mesh generation and physical quantity evaluation techniques are enabling technologies for geometry-based analysis techniques. The technologies implemented in GEOMESH are described herein.

### *Geometry Model*

A geometry model is composed of topological data and geometrical data. Topological data represents the relationship between topological entities such as the vertex, edge and face. Geometrical data defines the shape of topological entities using a geometrical entity such as a surface, polygon, line and curve. A simplified form of boundary representation (B-rep) is used for the topological data of a geometry model. Because of its generality, the boundary representation has been recently adopted in a broad range of applications in CAD/CAM/CAE industries.

A geometry entity defines the shape of a topological entity. The straight line and flat polygon are implemented as the primitive geometry entities. The shape of each loop is defined by a corresponding flat polygon. The mapping from a flat surface to a cylindrical surface is used for the modeling of a curved panel.

### *Mesh Generation*

GEOMESH can automatically generate meshes consisting of 3-D beam and shell elements using a mapped mesh approach. The mapped mesh generation consists of two steps: i) generation of super-elements for a geometry model; and ii) decomposition of these super-elements into finite elements. This approach generates a minimum number of high quality quadrilateral elements for a relatively regular geometry (which is typical in a aircraft structure).

In the current implementation, super-elements can be generated automatically only if the geometry model is composed of faces which are flat and parallel to the XY, YZ or ZX planes, and edges which are straight and parallel to the X, Y or Z axis. This is one of the major limitations in the current implementation. It will be addressed in the future.

**Mapped Mesh Approach** In the mapped mesh approach adopted in GEOMESH, each face of a geometry model is divided into super-elements. The shape of the super-elements is quadrilateral. A number of divisions is specified in each division direction. If the numbers of divisions are inconsistent among adjacent super-elements, quadrilateral elements generated from the mapping become inconsistent too. If a crack is located between adjacent super-elements, 2 nodes are generated at the same position for the formation of unconnected elements.

**Automatic Super-element Generation** GEOMESH can automatically generate super-elements when a geometry model is orthogonal. (i.e the model is composed of faces, which are flat and parallel to the XY, YZ or ZX planes, and edges, which are straight and parallel to the X, Y or Z axis.) Since the global damage tolerance model satisfies this condition, the super-element generation is fully automated.

An algorithm is implemented to create a 3-D orthogonal non-uniformly spaced grid for each part, so that each vertex of the part is placed on one of the grid points. Each face is then classified as to whether the face is parallel to the XY, YZ or ZX plane, and a 2-D cut plane which is coincident to the face is identified from the 3-D grid. The 2-D cut plane is a collection of rectangles. Rectangular

super-elements which are contained within the face are collected from the rectangles of the 2-D cut planes. Because all the super elements generated by the algorithms are rectangles, it is easy to define the number of divisions. If an average element size is specified, the AGILE mesh generator calculates the number of divisions for all the super elements. Then, it automatically generates shell and beam elements.

### *Evaluation of Analysis Result*

GEOMESH can evaluate analysis results at an arbitrary location independent of the locations of the nodes and elements, as if the analysis results were mapped on the geometry model rather than at each node or at each element integration point. The displacements of the beams are represented using free-form curves; and the displacements of the shells are represented using free-form surfaces.

A physical quantity at a given point is evaluated through : i) searching for the element that contains the given point; ii) calculating the local co-ordinate of this point in this element ; iii) calculating the value of the physical quantity by interpolation either from values at the nodes or at the element integration points using standard finite element interpolation techniques.

Note that this algorithm does not work if an evaluation point is coincident with the location of a crack, because it is ambiguous which side of the crack is chosen. Therefore, the evaluation point has to be placed a small distance apart from the crack.

**Displacement** Displacements are imported at each node in a finite element model. The displacements have 6 components, which consists of 3 translation components,  $u_x$ ,  $u_y$  and  $u_z$ , and 3 rotation components,  $\theta_x$ ,  $\theta_y$  and  $\theta_z$ . The distribution of the displacement is assumed to be linear over a 4 node quadrilateral shell element.

**Stress** In-plane element stress is imported at each integration point of each shell element. The local co-ordinate system of the element is used. the in-plane stress has 3 components,  $\sigma_{xx}$ ,  $\sigma_{xy}$  and  $\sigma_{yy}$ . The in-plane element stress is redistributed at each node to form an extrapolated nodal stress, so that the distribution of stress is smooth. Currently, this is implemented in the 1st order 4 node quadrilateral shell element. This element has one integration point at the center of the element. Therefore, the distribution of in-plane element stress is constant over the element. However, the distribution of extrapolated nodal stress is linear over the element.

**Reaction Force** GEOMESH uses beam elements to model stiffeners, rivets or rigid connections. A rivet force may be needed at the point where a rivet is directly connected to a skin to form free body diagrams.

A reaction force is calculated from the corresponding beam elements. For each beam element, a shear force is calculated from the displacements of the 2 nodes of the beam element.

### 2.3.3 Analysis Model and Feature Modeling

An *analysis model* is a geometry model with associated attributes relevant to a finite element analysis. Known as a *Product Model*<sup>2</sup> in the CAD industry, it is an intelligent CAD model with information and knowledge about the finite element analysis. An analysis model is a product model for the finite element analysis. It is the primary modular interface for the finite element analysis.

In general, the user can create an analysis model; interact with it; attach analysis conditions to it; and visualize analysis results on it. Because it is completely hidden behind the geometry model, the mesh is invisible from the user.

A *feature model* is a high level geometry model with built-in information of *model simplification*. It consists of a history list of geometry definition commands. Each command is an operation such as extrusion, fillet, cut-out, or so. A geometry model of a specified level of detail can be constructed from its command history list.

A feature-based model knows how to analyze itself and how to perform model simplification if necessary. It can generate an analysis model. It also knows how to transfer boundary conditions between analysis models of different levels of details.

The part and connection are the building blocks of a feature model. A feature model consists of parts and connections. A connection joins two parts to each other. Each part and connection contains a command history list to generate a geometry model of the most detailed level. By specifying the level of detail on each part connection, the feature model can produce a geometry model that is simplified to the given level of detail.

**Part** Two types of parts for feature models are implemented. They are: beam-like narrow parts and shell-like thin parts.

1. Beam-like narrow parts can produce a wire frame model of a beam structure or a surface model of a shell structure. The knowledge to transfer boundary conditions between two wire frame models, a wire frame model and a surface model, or two surface models has been implemented.
2. Shell-like thin parts can produce a surface model of shell structure. The knowledges to transfer boundary conditions between two surface models are implemented.

**Connection** Three types of connections are implemented. They are: riveted line, riveted area, and rigid connection. In a riveted line, parts are connected by equally spaced rivets. In a riveted area, parts are connected by a rectangular grid of rivets. The rectangle is perpendicular to the direction of the rivets.

---

<sup>2</sup> A product model is a CAD geometry model which contains application-specific information and intelligence to perform application-specific tasks.

### 2.3.4 Hierarchical Analysis Based on Feature Modeling

In an automated hierarchical analysis, only a single detailed feature model is required. The hierarchical analyzer automatically constructs the analysis models for each level of analysis with corresponding geometrical details and coverage. Thus, four major tasks are performed by the automated hierarchical analyzer. They are i) the simplification of geometry; ii) the extraction of subregions; iii) the evaluation of the analysis results in the current analysis; and iv) the construction of boundary conditions for the analysis in the next stage. These tasks are described in this section.

#### *Simplification of Geometry*

Simplification of geometry is necessary to reduce the number of D.O.F. required to construct a finite element model for a given feature model. The D.O.F.'s saved by simplifying unnecessary details can be allocated to the regions where mesh refinement can significantly affect the accuracy of the finite element analysis, such as the vicinity of a crack tip.

In general, simplification of geometry is the process of elimination of small scale dimensional parameters in the feature model. Small features can be eliminated without significant degradation in accuracy (except in the vicinity of the eliminated feature). For example, in case of an aircraft fuselage, dimensional parameters such as the radius of rivet holes in the skin, the size of MSD cracks, a joggle depth of stringers at the junction with tear straps, and the radius of fillets of a finger doubler can be ignored in a typical intermediate level model.

Narrow structures can be simplified as beams. If all the stiffeners are modeled as beams in a global model, the dimensional parameters in the same order or less than that of the width (or height) of the stiffeners are ignored from the feature model. The information is used to generate the geometrical properties of the beams.

The rivet distribution pattern heavily affects the number of D.O.F. required to model a finite element model. To reduce the number of D.O.F., rivet spacing can be artificially enlarged. At the same time, the geometrical property parameters of the rivets have to be modified accordingly.

Model simplification methods that have been implemented are i) modeling stiffeners as beams; ii) elimination of small features; iii) modeling rivets as beams; iv) simplification of rivet distributions; v) using rigid connections.

**Stiffener Modeled as a Beam** A narrow structure is defined by an extrusion operation in CAD geometry modeling. First, a geometry model of a cross-section is defined. Then, it is extruded along a path which defines the shape of the narrow structure. A solid model is generated from the extrusion of a surface; a surface model is generated from the extrusion of a wire frame; and a wire frame is generated from the extrusion of a point.

A stiffener is the extrusion of a section along a given path. It can be modeled as a 3D solid with a solid model, or as a shell structure with a surface model, or as a frame with a wire frame model. In order to simplify the stiffener as a shell structure, the thickness parameter is degenerated into a geometrical property of a surface model. In order to simplify the stiffener as a frame, the

cross-sectional parameter is degenerated into a geometrical property of a wire model. A feature model of the stiffener is implemented so that the automatic hierarchical analyzer can perform these model simplifications. Automatic mesh generators have been implemented to generate shell models and/or beam models. Since no solid mesh generator is implemented, no 3D solid model can be generated.

A wire frame model is used for a stiffener in a aircraft structure in a global analysis. It is discretized using beam elements in the corresponding finite element model.

**Elimination of a Small Feature** The complexity of a geometry model affects significantly the number of D.O.F. of the generated finite element model. Some of the small features can be ignored in a early stage of a hierarchical analysis, since the detailed stress solution nearby these features is not important. In the early stage of a hierarchical analysis, it is important to determine the accurate boundary conditions for the analysis in the next stage. These small features have an insignificant effect on the solution for the boundary condition; while accurate modeling of these features can significantly increase the number of D.O.F.

Filleting, tapering, making a small hole, or offsetting are examples of such small features. Even small curved edges can be considered as features, because the extra nodes needed to represent the curve can lead to a significant increase in the number of D.O.F. in the finite element model generated by the automated mesh generator.

Typically, the construction of a geometry model starts from a simple model. Smaller and smaller features are added incrementally to it. With a record of this procedure, a simplified model can be reproduced by a modification to the procedure.

**Rivet Modeling as a Beam** Beam elements are used to model the rivets. Swift's experimental equation is used to determine the stiffness of the rivets. They are

$$K_{axial} = \frac{ED^2\pi}{2(t_{s1} + t_{s2})} \quad (2.1)$$

$$K_{trans} = \frac{ED}{A + CD(1/t_{s1} + 1/t_{s2})} \quad (2.2)$$

where  $K_{axial}$  is the axial direction stiffness of the rivet ( $psi \cdot in$ ),  $K_{trans}$  is the transverse direction stiffness of the rivet ( $psi \cdot in$ ),  $E$  is the Young's modulus of the rivet ( $psi$ ),  $D$  is the diameter of the rivet ( $in$ ),  $t_{s1}$  is the thickness of sheet 1 ( $in$ ), and  $t_{s2}$  is the thickness of sheet 2 ( $in$ ).  $A$  and  $C$  are the coefficients in Swift's equation.  $A = 5.0$ ,  $C = 0.8$  for aluminum rivets; and  $A = 1.666$ ,  $C = 0.86$  for steel rivets.

The corresponding geometrical properties for the beam elements are defined as follows.

$$A = \frac{K_{axial}l}{E} \quad (2.3)$$

$$I = \frac{K_{trans}l^3}{3E} \quad (2.4)$$

where  $A$  is the cross sectional area ( $in^2$ ),  $I$  is the moment of inertia ( $in^4$ ), and  $l$  is the length of beam element of the rivet ( $in$ ).

**Simplification of the Rivet Distribution** A feature model of a rivet connection consists of a number of rows of rivets. These rows of rivets are distributed in a regular fashion. Multiple rivets can be combined and modeled by a single beam element, whose stiffness is the sum of these rivets. Multiple rows of rivets can be combined and modeled by a single row of beams. This simplification technique artificially enlarges the rivet spacing. Therefore, the number of D.O.F. in the finite element model can be reduced significantly. This is a very useful simplification technique for a earlier stage analysis of a build-up structure in a hierarchical analysis. In an extreme case, all the rivets in the feature model can be degenerated to a single beam element located at the center of the rectangle.

**Rigid Connection as a Collection of Rivets** The connection between a frame and a stringer, without a shear clip, is effectively a rigid connection. The geometrical details of such a connection are very complicated. Such a connection is modeled as a rigid connection, using very *strong* beams. The stiffness of the beam element is assigned by the program so that the beam element is so stiff that the relative translation and rotation between the two nodes are practically zero.

### *Subregion Extraction*

A subregion is automatically extracted for the subsequent models involved in a hierarchical analysis. A subregion can be of any shape. Typically it is rectangular. Usually, the subregion is contained completely inside the given model, from which the extraction is performed. However, the prescribed subregion can also intersect with the boundary of the given model. In this case, the boundary of the given model in the prescribed subregion becomes a part of the boundary in the extracted model. A CAD operation, *intersection operation*, is used to extract the geometrical model of the subregion.

### *Construction of Boundary Conditions*

The boundary conditions for the subsequent analysis are constructed using the analysis results evaluated at the locations of the boundaries in the current model. Once the subregion extraction is performed, the location of the boundaries in the current model is determined. Analysis results can be evaluated at these locations for the calculation of the boundary conditions for the analysis in the next stage.

The boundary conditions at the end of stiffeners are prescribed as displacement boundary conditions in the subsequent models generated by the automatic hierarchical analyzer. When a wire frame model of a stiffener is modeled in detail using a surface model in the next stage, the rotation and the displacement at this point is used to calculate the displacement constraints of the shell model at the end of the stiffener.



When the hierarchical analysis transitions from a 3D shell analysis to a 2D plane stress/strain analysis, it is necessary to perform a projection of the analysis result. For example, when a local region of the fuselage skin is to be analyzed by a 2D plane stress/strain analyzer (such as a code using a 2D finite element alternating method), conversion of analysis results for a 3-D shell to the corresponding boundary condition for a 2D analysis is required. In-plane displacements in the mid-plane are used for displacement boundary conditions; while membrane stresses in the mid-plane are used for the construction of traction boundary conditions.

## 2.4 Buckling Analysis of a Composite with/without delamination

The primary damage in a structure loaded in compression which must be considered during design is a hole (Fig. 2.12). For laminated composites, delaminations will also be of relevance. It is to be expected [with some preliminary results that confirm these expectations being reported in Vellaichamy, et. al (1990)] that the buckling load of a panel, with a hole, in compression will depend on the shape and the size of the hole. The buckling load of a panel with an elliptical hole whose major axis is aligned with the direction of compression can be expected to be lower than that with a circular hole of the same area. Further, it is expected that for an elliptical hole of a given area, the buckling load will decrease with an increase in the aspect ratio of the ellipse, as long as the major axis of the ellipse is aligned with the direction of compression. In the limit as the elliptical hole shrinks to a crack whose axis is parallel to the direction of compression, with the slightest imperfection, the crack may propagate in mode III in post-buckling deformation. Such mode III behavior would severely affect the structural integrity. BUCKDEL, as developed primarily in Phase I of this SBIR project, can be used to compute the buckling and post-buckling response of a stiffened structure containing damage in the form of holes and delaminations of arbitrary shape. In addition, it computes the pointwise energy release rate around the delamination front. In future work, the ability to treat the mode III crack problem will be added to BUCKDEL.

A brief overview of BUCKDEL is given here. For more details, see the Users and Theory Manuals of BUCKDEL, which are parts of the final report for Phase I of this project. BUCKDEL was developed as a stand-alone program in Phase I of this project. It was connected with ASTROS as a linear buckling analysis module in Phase II.

BUCKDEL uses a multi-domain method to model delaminations of arbitrary shape. In this method, the delaminated shell is assumed to be assembled with three regions-(1) Undelaminate: undelaminated zone; (2) Delaminate: thinner side of the delaminated zone and (3) Base: thicker side of the delaminated zone. Transverse shear deformation plays an important part in the case of composite structures, hence, it is introduced explicitly and the assumptions of the Reissner-Mindlin theories of plate bending are used for modeling each region of the multi-domain model. Thus, for each region, the 3-dimensional displacement field ( $\mathbf{U} \equiv \{U_1 \ U_2 \ U_3\}$ ) is expressed in terms of the corresponding mid-surface displacement ( $\mathbf{u} \equiv \{u_1 \ u_2 \ u_3\}$ ) and rotation ( $\theta \equiv \{\theta_1 \ \theta_2 \ 0\}$ ) fields as,

$$\mathbf{U}^{(i)}(x_\alpha, x_3) = \mathbf{u}^{(i)}(x_\alpha) - x_3^{(i)} \theta^{(i)}(x_\alpha) \quad (2.5)$$

where  $x_\alpha^{(i)}$  ( $\alpha = 1, 2$ ) are the inplane curvilinear shell coordinates and  $x_3^{(i)}$  is the thickness coordinate

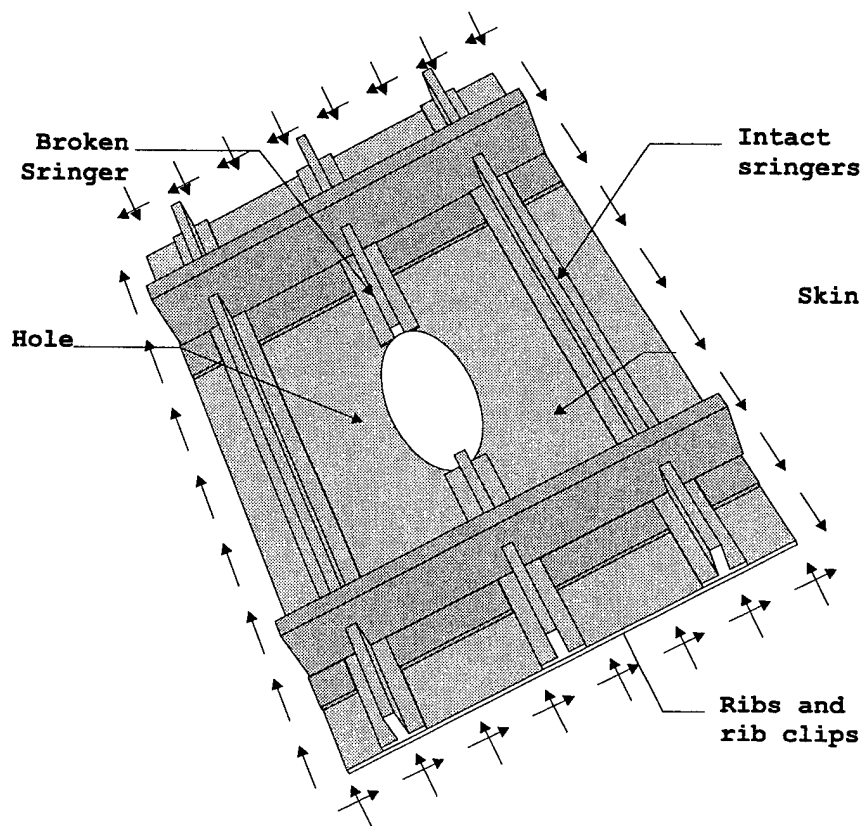


Figure 2.12: Damage in the Upper (Compression) Skin of a Wing

for the  $i^{th}$  ( $i = 1, 2, 3$ ) shell. The structural continuity at the delamination front  $\Gamma$  is maintained by assuming the deformation to be unique at the junction of the three shells i.e.  $\mathbf{U}^{(1)} = \mathbf{U}^{(2)} = \mathbf{U}^{(3)}$  on  $\Gamma$  in accordance with the Reissner-Mindlin law of flexure (Eq. (2.5)). In other words, *at the delamination edge*, the mid-surface degrees of freedom of the delaminate and the base shells are assumed to be related to those of the undelaminated shell by,

$$\begin{pmatrix} u_3^{(1)} & = & u_3^{(2)} & = & u_3^{(3)} \\ \theta_\alpha^{(1)} & = & \theta_\alpha^{(2)} & = & \theta_\alpha^{(3)} \\ u_\alpha^{(i)} & = & u_\alpha^{(1)} & + & h^{(i)}\theta_\alpha^{(1)} \end{pmatrix}_{at \Gamma} \quad (2.6)$$

where  $h^{(i)}$  is the distance of the midsurface of the  $i^{th}$  shell from the laminate midsurface.

Each lamina is assumed to be orthotropic, and the inplane stresses  $\sigma^{(i)} = \{\sigma_{11} \sigma_{22} \sigma_{12}\}^{(i)}$  and the transverse shear stresses  $\tau^{(i)} = \{\tau_{13} \tau_{23}\}^{(i)}$  are related to the linear components of the membrane strain  $\epsilon^{(i)} = \{\epsilon_{11} \epsilon_{22} \epsilon_{12}\}^{(i)}$ ; nonlinear components of the membrane strain  $v^{(i)} = \{v_{11} v_{22} v_{12}\}^{(i)}$ ; flexural strain due to mid-surface rotation  $\kappa^{(i)} = \{\kappa_{11} \kappa_{22} \kappa_{12}\}^{(i)}$ ; flexural strain due to transverse shear strain  $\chi^{(i)} = \{\chi_{11} \chi_{22} \chi_{12}\}^{(i)}$  and transverse shear strains  $\gamma^{(i)} = \{\gamma_{13} \gamma_{23}\}^{(i)}$  as

$$\begin{Bmatrix} \sigma \\ \tau \end{Bmatrix}^{(i)} = \begin{bmatrix} E_{11} & E_{12} & E_{16} & 0 & 0 \\ E_{12} & E_{22} & E_{26} & 0 & 0 \\ E_{16} & E_{26} & E_{66} & 0 & 0 \\ 0 & 0 & 0 & E_{44} & E_{45} \\ 0 & 0 & 0 & E_{45} & E_{55} \end{bmatrix}^{(i)} \begin{Bmatrix} (\epsilon + v) + x_3(\kappa + \chi) \\ \frac{1}{2}\gamma \end{Bmatrix}^{(i)} \quad (2.7)$$

where the material constitutive terms  $E_{ij}^{(i)}$  are functions of the thickness coordinate of each shell  $x_3^{(i)}$ . Generally, for a laminate with orthotropic layers,  $E_{ij}^{(i)}$  are assumed to be piecewise constants over the laminate thickness.

Integrating along the thickness, the constitutive equations can be written in terms of the inplane stress resultants  $\mathbf{N} \equiv \{N_{11} N_{22} N_{12}\}$ , bending moments  $\mathbf{M} \equiv \{M_{11} M_{22} M_{12}\}$ , and transverse shear stress resultant  $\mathbf{Q} \equiv \{Q_{13} Q_{23}\}$ , for each region of the multi-plate model as,

$$\begin{Bmatrix} \mathbf{N} \\ \mathbf{M} \\ \mathbf{Q} \end{Bmatrix}^{(i)} = \begin{bmatrix} \mathbf{A} & \mathbf{B} & \mathbf{0} \\ \mathbf{B} & \mathbf{D} & \mathbf{0} \\ \mathbf{0} & \mathbf{0} & \mathbf{G} \end{bmatrix}^{(i)} \begin{Bmatrix} (\epsilon + v) \\ (\kappa + \chi) \\ \gamma \end{Bmatrix}^{(i)} \quad (2.8)$$

where

$$\begin{aligned} (A_{kl}; B_{kl}; D_{kl})^{(i)} &= \int_{t_i} E_{ij}^{(i)}(x_3) (1; x_3; x_3^2) dx_3 \\ G_{mn}^{(i)} &= \int_{t_i} s_m s_n E_{ij}^{(i)}(x_3) dx_3 \end{aligned}$$

In addition to a beam element, BUCKDEL implements a three noded triangular curved shell element. The shell element is described in the curvilinear coordinate system  $x - y$  and the area

coordinates are used for the field-description. Accordingly we have,

$$\{x \ y \ 1\} = \sum_{i=1}^3 L_i \{x \ y \ 1\}_i \quad (2.9)$$

Inverting the above relationship, we get,

$$L_i = \frac{1}{2\Delta} (a_{i1}x + a_{i2}y + a_{i3}) \quad (2.10)$$

where

$$a_{i1} = y_j - y_k; \quad a_{i2} = x_k - x_j; \quad a_{i3} = x_j y_k - x_k y_j$$

$$\Delta = \frac{1}{2} (x_2 y_3 - x_3 y_2 + x_3 y_1 - x_1 y_3 + x_1 y_2 - x_2 y_1)$$

and  $j = 2, 3, 1$ ;  $k = 3, 1, 2$  as  $i = 1, 2, 3$ .

The inplane displacements and the transverse shear strains need to satisfy  $C^0$ -continuity while the transverse deflection needs to satisfy  $C^1$ -continuity in the present formulation. The independent field variables  $u, v, w, \gamma_{xz}$  and  $\gamma_{yz}$  are expressed in terms of the nodal degrees of freedom  $u_i, v_i, w_i, \rho_{x_i} \equiv (-w_{,y})_i, \rho_{y_i} \equiv (w_{,x})_i, \gamma_{xz_i}$  and  $\gamma_{yz_i}$  as,

$$\{u \ v \ \gamma_{xz} \ \gamma_{yz}\} = \sum_{i=1}^3 L_i \{u \ v \ \gamma_{xz} \ \gamma_{yz}\}_i$$

$$w = \sum_{i=1}^3 (N_{1i} w_i + N_{2i} \rho_{x_i} + N_{3i} \rho_{y_i}) \quad (2.11)$$

where

$$N_{1i} = L_i + L_i^2 L_j + L_i^2 L_k - L_i L_j^2 - L_i L_k^2$$

$$N_{2i} = a_{k1} \left( L_i^2 L_j + \frac{1}{2} L_i L_j L_k \right) + a_{j1} \left( L_i^2 L_k + \frac{1}{2} L_i L_j L_k \right)$$

$$N_{3i} = a_{k2} \left( L_i^2 L_j + \frac{1}{2} L_i L_j L_k \right) + a_{j2} \left( L_i^2 L_k + \frac{1}{2} L_i L_j L_k \right) \quad (2.12)$$

are the cubic polynomials for the transverse deflection.

In the above element formulations, the inter-element  $C^0$ -continuity is exactly satisfied for all the field variables. However, the inter-element  $C^1$ -continuity required for the transverse deflection, in case of a shell element, is satisfied *a posteriori* in a weak form using the Hu-Washizu variational principle.

BUCKDEL uses an automated method to follow the post-buckling paths of the damaged structure. The automated post-buckling solution involves: detection of a possible instability in the solution and elimination of possible path-retracing; classification of the detected instabilities; and computation of the post-through buckling solution(s). Solution instabilities are detected by monitoring the rank of the tangent stiffness matrix. Whenever the determinant of the tangent stiffness

matrix changes its sign, the solution senses possible instabilities in that range of load and changes the sign of the next load increment to avoid path-retracing. Through a cycle of iterations, the location of instabilities are identified as the load levels for which the tangent stiffness becomes singular. The tangent stiffness is often *scaled* to minimize numerical errors. The identified instability points are then classified as limit points or bifurcation points using some simple and cost-effective rules [Huang and Atluri (1995)]. If the instability point is a limit point, the *arc-length continuation* is enough to obtain the post-buckling solution path. However, if the instability point happens to be a bifurcation point, the strategies described in detail in Huang and Atluri (1995) are used to trace the appropriate post-buckling solution branch. The nonlinear fundamental state between the two solution points  $n - 1$  and  $n$  in the neighborhood of the bifurcation point is *linearized* to obtain the *asymptotic* solution for obtaining an approximate critical buckling load factor. A linear combination of the *normalized* eigen-vector associated with the critical buckling load factor and its orthogonal counterpart is used to determine the initial post-buckling paths.

## 2.5 Finite Element Alternating Method

The Schwartz-Neumann alternating method is based on the superposition principle. The solution on a given domain is the sum of the solutions on two other overlapping domains, with part of the boundary conditions as unknowns. The alternating method can be viewed as the fixed point iteration scheme used to solve these unknown boundary conditions. Based on this point of view, we can perform a convergence study. The alternating method converges unconditionally when there are only traction boundary conditions specified on the body. The convergence criterion for mixed boundary value problems, where there are applied displacement boundary conditions as well as traction boundary conditions, is discussed in the following. Compare the work done by the applied forces in the following two cases. In the first case, arbitrary displacement conditions exist on the surfaces of the cracks in the cracked finite body, while all the boundary conditions elsewhere are replaced by homogeneous boundary conditions, i.e. remove all tractions and reduce all the applied displacements to zero magnitude. In the second case, the same displacement conditions exist on the surfaces of the cracks in the infinite domain. If the work done in the cracked finite body is always smaller than twice the work done in the infinite domain, then the alternating method converges. Otherwise, it does not. For most practical problems, this ratio is close to one. Thus, the alternating method converges rapidly, as discussed in detail in the following section.

### 2.5.1 Superposition Principle and the Alternating Method

Consider  $n$  cracks in a body of finite size. The crack surfaces which are traction free, are denoted collectively as  $\Gamma_c$ . Let the boundary of the finite domain(not including the crack surface) be  $\Gamma$ , of which the boundary with prescribed tractions  $t^o$  is  $\Gamma_t$ , and the boundary with prescribed displacements  $u^o$  is  $\Gamma_u$ . It is clear that  $\Gamma = \Gamma_u \cup \Gamma_t$ .

The alternating method uses the following two simpler problems to solve the original one. The

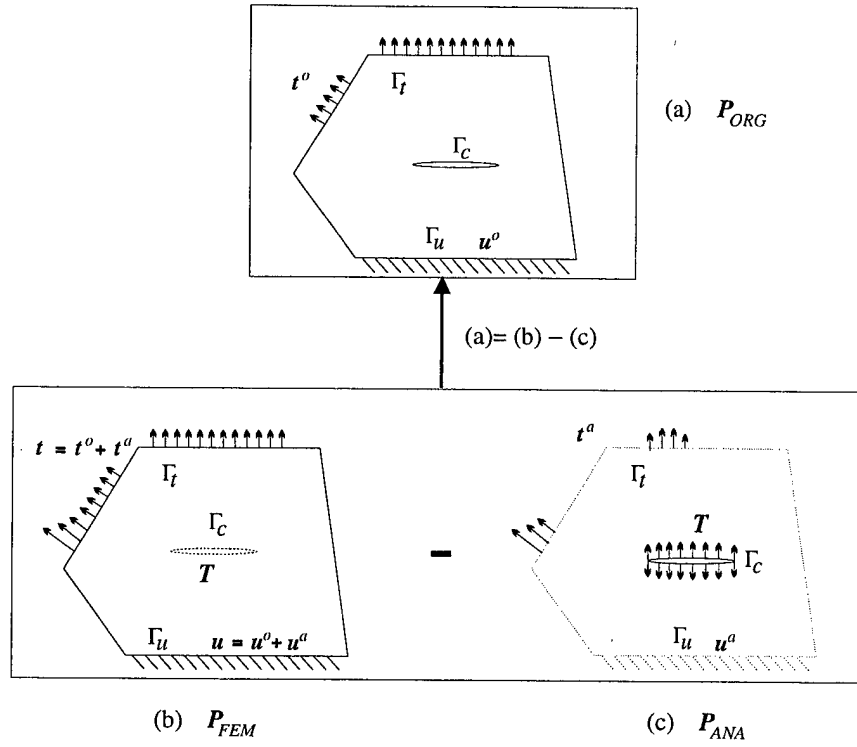


Figure 2.13: Superposition Principle for Finite Element Alternating Method

first one, denoted as  $P_{ANA}$  [shown<sup>3</sup> in Fig. 2.13(c)], is that of the same  $n$  cracks in the infinite domain subjected to the unknown crack surface loading  $T$ . The second one, denoted as  $P_{FEM}$  [shown in Fig. 2.13(b)], has the same finite geometry as in the original problem except that the cracks are ignored. The boundary  $\Gamma_u$  of  $P_{FEM}$  has the prescribed displacement  $u$ , while the boundary  $\Gamma_t$  has the prescribed traction  $t$ . The prescribed displacements and tractions are different from those in the original problem in general. Because of the absence of the cracks, the problem  $P_{FEM}$  can be solved much easier by the finite element method (or the boundary element method).

To solve the original problem,  $P_{ORG}$  (shown in Fig. 2.13(a)), the crack surface loading  $T$ , the prescribed displacement  $u$  and the traction  $t$  must be found such that the superposition of the two alternative problems  $P_{ANA}$  and  $P_{FEM}$  yields the original one,  $P_{ORG}$ . The detailed procedures to find these boundary conditions are described in the following.

In the uncracked body problem  $P_{FEM}$ , the tractions  $T$  at the location of the cracks in the cracked body  $P_{ORG}$  can be solved, for any given boundary loads  $u$  and  $t$ , using the finite element method. Due to the linearity of the problem, the solution can be denoted as

$$T = K^u u + K^t t \quad (2.13)$$

where  $K^u$  and  $K^t$  are linear operators.

<sup>3</sup> Fig. 2.13 only illustrates one crack. Many cracks may be present.

Similarly, the tractions  $t^a$  on boundary  $\Gamma_t$  and the displacements  $u^a$  on boundary  $\Gamma_u$  can be found in the infinite domain  $P_{ANA}$  for the given crack surface load  $T$ , which is the same as the crack surface traction obtained in the  $P_{FEM}$ . The solution can be denoted as

$$u^a = \overline{K}^u T \quad (2.14)$$

$$t^a = \overline{K}^t T \quad (2.15)$$

where  $\overline{K}^u$  and  $\overline{K}^t$  are also linear operators. Subtract the solution for  $P_{ANA}$  from the one for  $P_{FEM}$ . The resulting solution has zero tractions at the location of the crack surfaces. To ensure that the resulting solution has the same boundary conditions on  $\Gamma$ , the Eq. (2.16) and Eq. (2.17) must be satisfied.

$$u = u^o + u^a \quad (2.16)$$

$$t = t^o + t^a \quad (2.17)$$

The unknown tractions  $T$ ,  $t$  and unknown displacement  $u$  can be solved using these equations [Eq. (2.13) through Eq. (2.17)]. Eliminate  $u$ ,  $u^a$  and  $t$ ,  $t^a$  by substituting Eq. (2.16), Eq. (2.17), Eq. (2.14) and Eq. (2.15) into Eq. (2.13) to obtain the following equation for the traction  $T$ .

$$\left[ I - \left( K^u \overline{K}^u + K^t \overline{K}^t \right) \right] T = (K^u u^o + K^t t^o) \quad (2.18)$$

Eliminate  $u^a$ ,  $t^a$  and  $T$  to obtain the following equation for the unknown traction  $t$  and unknown displacement  $u$ .

$$(I - A) \begin{Bmatrix} u \\ t \end{Bmatrix} = \begin{Bmatrix} u^o \\ t^o \end{Bmatrix} \quad (2.19)$$

where

$$A = \begin{bmatrix} \overline{K}^u K^u & \overline{K}^u K^t \\ \overline{K}^t K^u & \overline{K}^t K^t \end{bmatrix}$$

and  $I$  is the identity operator.

Similarly, we can obtain the following linear system for traction  $t^a$  and displacement  $u^a$ .

$$(I - A)X = Y \quad (2.20)$$

where

$$X = \begin{Bmatrix} u^a \\ t^a \end{Bmatrix}$$

$$Y = A \begin{Bmatrix} u^o \\ t^o \end{Bmatrix} = \begin{bmatrix} \overline{K}^u K^u & \overline{K}^u K^t \\ \overline{K}^t K^u & \overline{K}^t K^t \end{bmatrix} \begin{Bmatrix} u^o \\ t^o \end{Bmatrix}$$

It is possible to solve these equations directly to obtain the tractions  $T$ ,  $t$  and displacement  $u$ . But this involves the evaluation of  $K^u$  and  $K^t$ , which requires solving the traction  $T$  at the location of the uncracked body subjected to all different loading patterns  $u$  and  $t$ . We have to solve the uncracked body problem a larger number of times, of the same order as that of the total number of

degrees of freedom of the boundary nodes, using the finite element method. Thus, it can be very expensive to find  $X$  by solving directly the linear system  $(I - A)X = Y$ . A fixed point iteration scheme can be used to solve this linear system. The iterative scheme can be devised as:

$$X^{(i+1)} = AX^{(i)} \quad i = 0, 1, 2, \dots, \infty \quad (2.21)$$

where  $X^{(0)} = \{u^o, t^o\}^T$ . If this procedure converges, the solution is

$$X = \sum_{i=1}^{\infty} X^{(i)}$$

Since

$$A = \begin{Bmatrix} \overline{K^u} \\ \overline{K^t} \end{Bmatrix} \cdot \{ K^u, K^t \}$$

the iterative scheme Eq. (2.21) is equivalent to the following alternating scheme

$$T^{(i)} = K^u u^{(i)} + K^t t^{(i)} \quad (2.22)$$

$$\begin{Bmatrix} u^a \\ t^a \end{Bmatrix}^{(i+1)} = \begin{Bmatrix} \overline{K^u} \\ \overline{K^t} \end{Bmatrix} T^{(i)} \quad (2.23)$$

for  $i = 0, 1, 2, \dots, \infty$ . In this case, the uncracked body problem is solved only a few times, because this fixed point iteration scheme converges quickly for practical problems. Therefore, the alternating method is much more efficient than solving the linear system directly. But it should be noticed that it may not be necessary to use the alternating method in some cases. It can be more efficient and accurate to solve directly when multiple crack solutions are constructed from that for a single crack. This will be discussed in detail in a later section.

### 2.5.2 Convergence of the Alternating Method

First it is shown that  $I - A$  is not singular and the linear system Eq. (2.20) has a unique solution. Suppose  $I - A$  is singular. Then, there must exist a *non-zero*  $X$  such that  $(I - A)X = 0$ , which means that there exist non-zero  $u^a$  and  $t^a$ , and therefore a non-zero  $T$ , such that

$$T = K^u u^a + K^t t^a$$

$$u^a = \overline{K^u} T$$

$$t^a = \overline{K^t} T$$

In this case the analytical solution and the finite element solution have the same displacement  $u^a$  on boundary  $\Gamma_u$  and the same traction  $t^a$  on boundary  $\Gamma_t$ . Subtracting the analytical solution from the FEM solution, we obtain the solution for the following problem. The entire boundary  $\Gamma$  is free of external loadings as well as the crack surfaces. But, the FEM solution gives zero displacements for the crack surfaces, while the analytical solution gives non-zero displacements for the crack



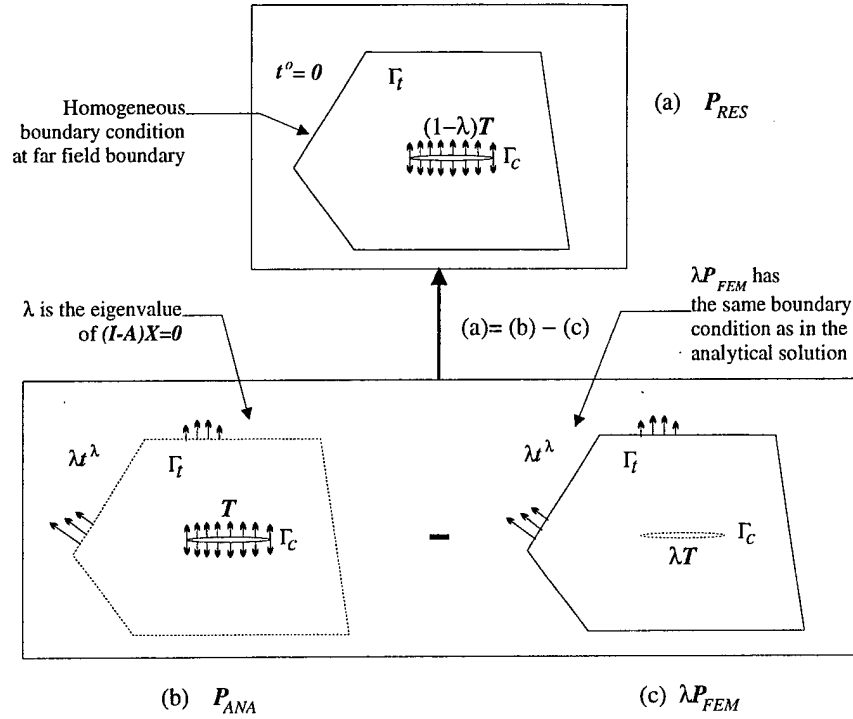


Figure 2.14: Subtract  $\lambda P_{FEM}$  from  $P_{ANA}$  to Obtain the Solution for  $P_{RES}$  which has Homogeneous Boundary Condition on  $\Gamma$

surfaces because of the non-zero  $T$ . Thus, the resulting solution has non-zero displacements at the crack surfaces. This is a contradiction because the cracks cannot be opened without any external load. Consequently,  $I - A$  is not singular.

The fixed point iteration scheme Eq. (2.21) converges if all the eigenvalues of  $A$  are in the open interval  $(-1, 1)$ . The scheme of Eq. (2.21) converges since the eigenvalues of  $A$  are in  $(-1, 1)$  for most problems of practical interest. The eigenvalues of  $A$  are smaller than 1. Let  $X_\lambda$  be an eigenvector of  $A$  corresponding to the eigenvalue  $\lambda$ .

$$T = K^u(u^\lambda) + K^t(t^\lambda)$$

$$\lambda u^\lambda = \bar{K}^u T$$

$$\lambda t^\lambda = \bar{K}^t T$$

The solution  $P_{RES}$ , shown in Fig. 2.14(a), is obtained by subtracting  $\lambda$  times the FEM solution (Fig. 2.14(c)) from the analytical solution (Fig. 2.14(b)). Here,  $u = 0$  and  $t = 0$  on  $\Gamma$  and the crack surface loading is  $(1 - \lambda)T$ , while the displacements at the crack surfaces are the same as those in the analytical solution. If the work done in opening the cracks in the infinite domain is  $W$ , the work done in opening the cracks in the finite domain (with the boundary condition  $u = 0$  and  $t = 0$ ) is  $(1 - \lambda)W$ , which is equal to the strain energy stored in the body. It must be positive. Thus,  $\lambda < 1$ .

It can be shown that  $\lambda \geq 0$  in the absence of the prescribed displacement boundary conditions. In this case, the resulting solution from the subtraction has zero tractions at the boundary  $\Gamma$ . Apply additional load  $\lambda t$  to the boundary  $\Gamma$  with the crack surfaces fixed. The stress state in the body will be the same as that in the analytical solution described above, after this additional loading is applied. This procedure of adding load on the boundary  $\Gamma$  is exactly the same as that in the FEM solution for the uncracked body, except that the load level is  $\lambda$  times that in the FEM solution, because the crack surfaces are fixed. Therefore, the work done by the additional load is positive. Consequently,  $(1 - \lambda)W < W$  and  $\lambda > 0$ . So, the alternating method converges for cracks in finite domains with arbitrary shapes and arbitrary *traction* boundary conditions.

In general, the eigenvalue  $\lambda$  can be smaller than zero for mixed boundary problems. It is greater than -1 only if  $(1 - \lambda)W < 2W$ . Thus, the convergence criterion for the alternating method for the general case with *mixed* boundary conditions can be stated as follows. The alternating method [Eq. (2.21)] converges if the crack surface loads do less work in the finite domain, with the homogeneous boundary condition  $u = 0$  and  $t = 0$  on  $\Gamma$ , than twice as much as they do in the infinite domain for *any* arbitrary distribution of crack surface displacements (see Fig. 2.15).

Quick convergence can be expected for most of the practical applications. For any crack surface displacements, the displacements and stresses at a point decay rapidly as the point moves away from the cracks. Thus, the work done in the finite domain with the homogeneous boundary condition is very close to the work done in the infinite domain. This implies that the eigenvalues of  $A$  are very small and the fixed point iteration converges rapidly. Indeed, all the mixed boundary value problems we have solved (for both 2D and 3D problems) to date using the finite element alternating method have converged.

### 2.5.3 Summary of FEAM Procedure

The alternating procedure defined in Eq. (2.21) can be translated into the following simple procedure. Refer to Fig. 2.13.

1. Solve  $P_{FEM}$  with the given load on the boundary  $\Gamma$ . Solve for the tractions, which are used to close the cracks. Denote the solution as  $S_1^{FEM}$ , where 1 indicates that this is the solution for the first iteration.

$$S_1^{FEM}: T^{(1)} = K^u u^o + K^t t^o$$

2. *Reverse* the crack surface traction obtained in the previous step and apply it as the load on the crack surfaces and solve the  $P_{ANA}$ . Denote the solution as  $S_1^{ANA}$ .

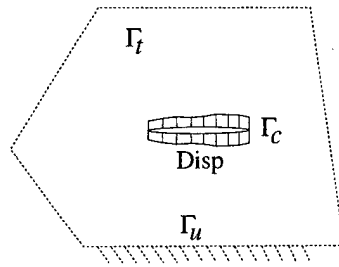
$$-S_1^{ANA}: \begin{Bmatrix} u \\ t \end{Bmatrix}^{(1)} = \begin{Bmatrix} \overline{K^u} \\ \overline{K^t} \end{Bmatrix} T^{(1)}$$

3. Find the tractions on the boundary  $\Gamma_t$  and the displacements on the boundary  $\Gamma_u$  from the analytical solutions obtained in the previous step. *Reverse* them as the load for  $P_{FEM}$ . Find the crack closing tractions from the solution  $S_2^{FEM}$ .

$$S_2^{FEM}: T^{(2)} = K^u u^{(1)} + K^t t^{(1)}$$

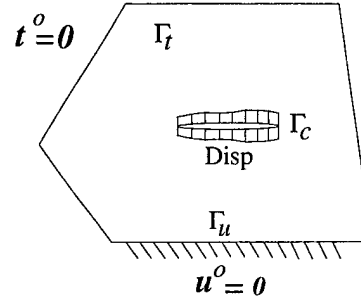
**FEAM converges**  
**if the work done in  $P_{FINITE}$  is**  
**less than twice of the work done in  $P_{INF}$**

the infinite body with any  
arbitrary crack surface  
displacement



(a)  $P_{INF}$

the finite body with the  
same crack surface  
displacement



(b)  $P_{FINITE}$

Figure 2.15: Convergence Criterion

4. Repeat steps 2 and 3 until the residual load is small enough to be ignored.

$$\begin{aligned} -S_i^{ANA}: \quad & \begin{Bmatrix} u \\ t \end{Bmatrix}^{(i)} = \begin{Bmatrix} \overline{K^u} \\ \overline{K^t} \end{Bmatrix} T^{(i)} \\ S_{i+1}^{FEM}: \quad & T^{(i+1)} = K^u u^{(i)} + K^t t^{(i)} \end{aligned}$$

for  $i = 2, 3, \dots$

The solution to the original problem is the summation of all those obtained in the alternating procedure, i.e.

$$S = \sum_{i=1}^n (S_i^{FEM} + S_i^{ANA}) \quad (2.24)$$

#### 2.5.4 2D FEAM for straight cracks

The analytical solutions for a crack in an infinite body, subjected to piecewise linear crack surface traction [Wang and Atluri(1996)], is used for the construction of the 2D FEAM for straight cracks in a finite sheet. Since the Finite Element Alternating Method is based on the superposition principle, the complicated rivet force exerted on the skin by the rivets can be easily taken into

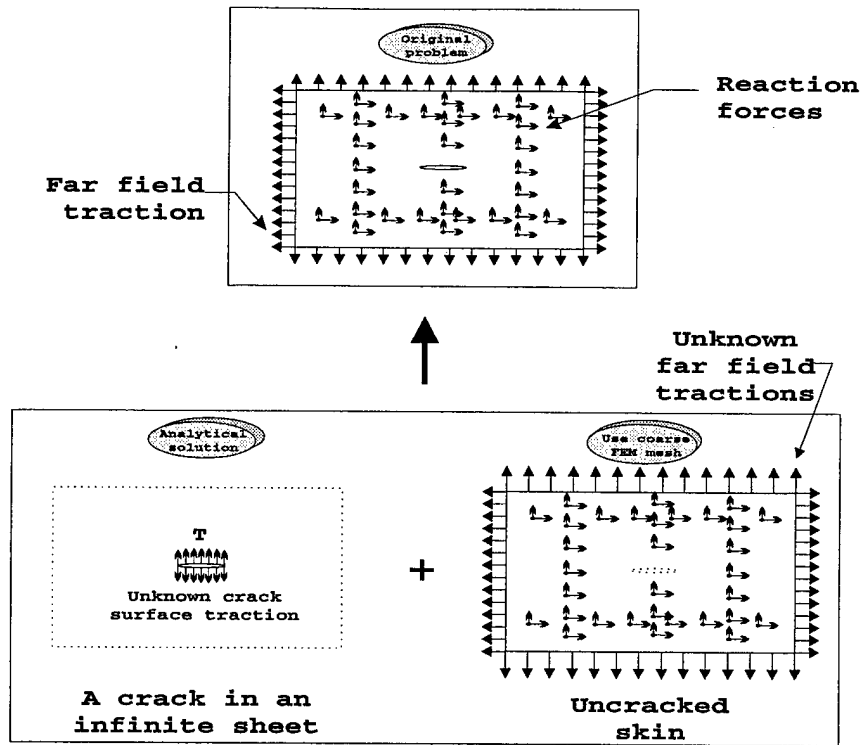


Figure 2.16: Superposition Principle Used in the Finite Element Alternating Method

account. Consider the local model of the isolated cracked skin [see Fig. 2.11]. The skin is being subjected to far-field tractions, and the stiffener to reaction forces. The stress-intensity factors for single or multiple cracks (including Widespread Fatigue Damage) in the skin can be determined in the local analysis using the Finite Element Alternating Method (FEAM), while still using a coarse finite element mesh. The problem in Fig. 2.11 can be solved with the FEAM depicted in Fig. 2.16, wherein it can be seen that the problem of Fig. 2.11, can be identified with the problem labeled as the “original problem” in Fig. 2.16.

Essentially, it is a fixed point iteration scheme which solves the superposition of the following two problems[see Fig. 2.16].

1. the uncracked, finite-sized skin subjected to external loads (including the reaction forces exerted by the stiffeners on the skin) and unknown external boundary loads;
2. a crack in an infinite sheet subjected to a crack surface traction

The crack surface traction in the infinite sheet cancels out the cohesive traction at the location of the crack in the first problem; while the unknown external boundary loads in the first problem cancel out the tractions at the same location in the second problem. Thus, the original problem, i.e. a cracked sheet of a finite dimension subjected to reaction forces exerted by the stiffeners with other boundary loadings, is exactly the superposition of these two problems.

The FEAM is used to solve this superposition problem. First, reverse the cohesive tractions at the location of the crack in the finite element model of the uncracked skin and use them as the load acting on the crack in an infinite sheet. Then, reverse the residuals at the locations of the far field boundaries in the infinite sheet and apply them as loads acting on the boundaries of the uncracked skin. In this way, the cohesive tractions at the location of the cracks and the residuals at the locations of the external boundaries are corrected iteratively. This procedure converges very fast, usually in two or three iterations. A flow chart illustrating the FEAM is shown in Fig. 2.17.

Fracture mechanics parameters can be found accurately because the near crack tip fields are captured exactly by the analytical solutions. Coarser meshes can be used in the finite element analysis because the cracks are not modeled explicitly. The finite element method is only used to compute the cohesive tractions at the crack location, which has a smooth distribution. Therefore, a very coarse mesh can be used. Fig. 2.18 shows typical finite element meshes around the crack tip, when a) the Equivalent Domain Integral (EDI) based method is used to evaluate stress intensity factors; or, b) the FEAM is used. In Fig. 2.18, the EDI based method also uses singular quarter-point elements. The simplicity of the FEAM mesh relative to the EDI mesh, which must explicitly model crack tips is apparent from this figure.

In a parametric analysis of various crack sizes, such as is necessary in fatigue calculations, the stiffness matrix of the finite element model is decomposed only once, since the stiffness of the uncracked structure remains the same for all crack sizes. In the other approaches, such as those using singular/hybrid type special crack-tip finite elements or EDI methods, the cracks must be modeled explicitly. Therefore, the global stiffness matrix must be computed and decomposed for each crack size. Thus, the FEAM is very efficient in terms of both computational time and human effort (i.e. mesh generation) when applied to problems such as fatigue crack growth.

Finally, it is noted that a simple superposition method can be used to construct the solution for multiple cracks in an infinite domain, subjected to arbitrary crack surface tractions, using the solution for a single crack in an infinite domain (see the Appendix for theoretical details). With the solution for multiple cracks in an infinite domain, the FEAM can be used to solve problems of multiple cracks with arbitrary crack lengths and orientations at arbitrary locations. This is particularly useful in the treatment of Widespread Fatigue Damage (WFD).

### ***2.5.5 3D FEAM for surface flaws and corner cracks***

The analytical solution for an embedded elliptical crack in an infinite body, subjected to arbitrary crack face tractions [Vijayakumar and Atluri (1981)], is used to construct the 3D FEAM for surface flaws and corner cracks. A 20-node second order brick element is used in the 3D FEAM module.

The finite element method is used to analyze the uncracked solid. Non-zero stresses are calculated at the location of the actual crack. These stresses must be removed in order to create a traction free crack as in the actual problem. The infinite body with an embedded crack has a solution which is valid for an arbitrary distribution of tractions on the crack face. The detailed steps involved in the FEAM for a crack in a finite body are as follows.

1. Solve the uncracked finite body under the given external loads using the finite element

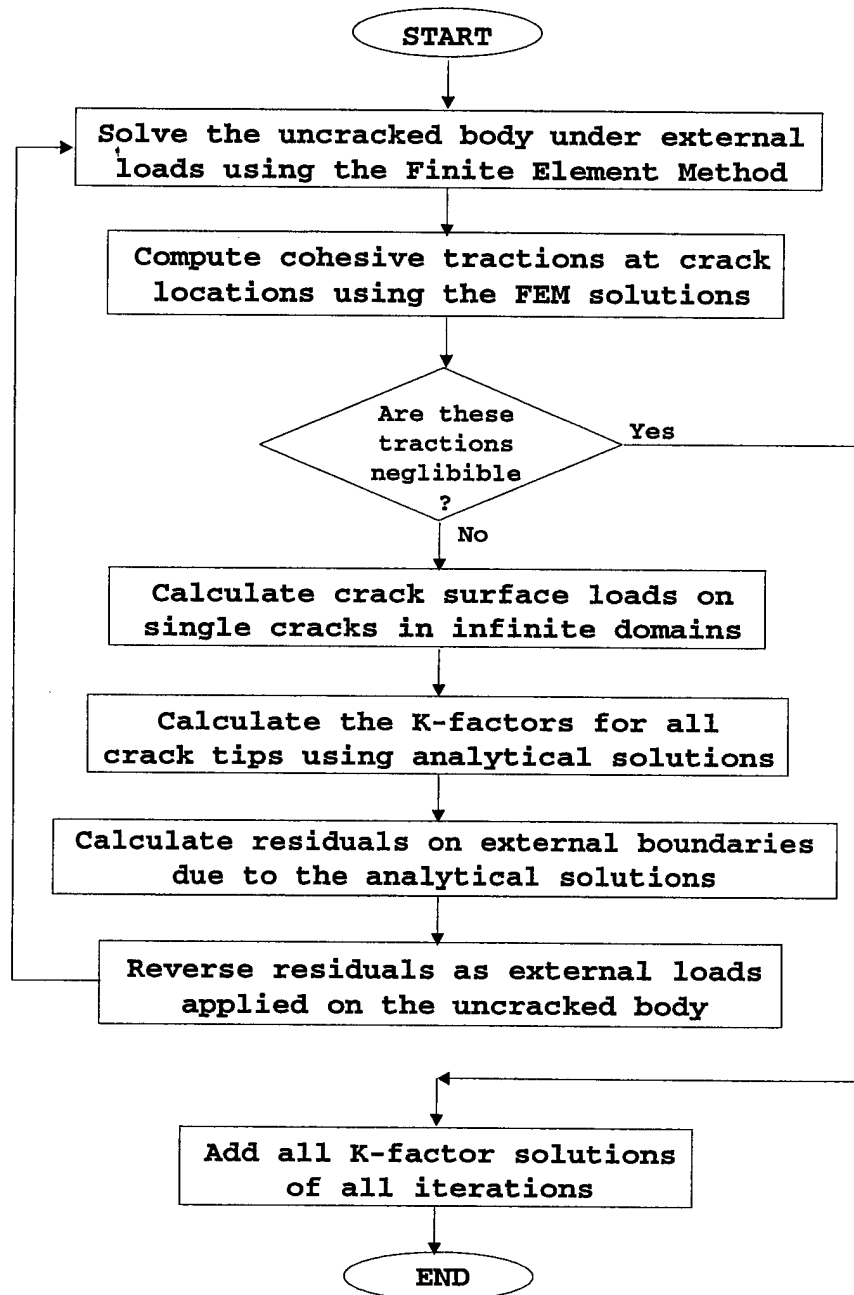


Figure 2.17: Flow Chart of the Finite Element Alternating Method

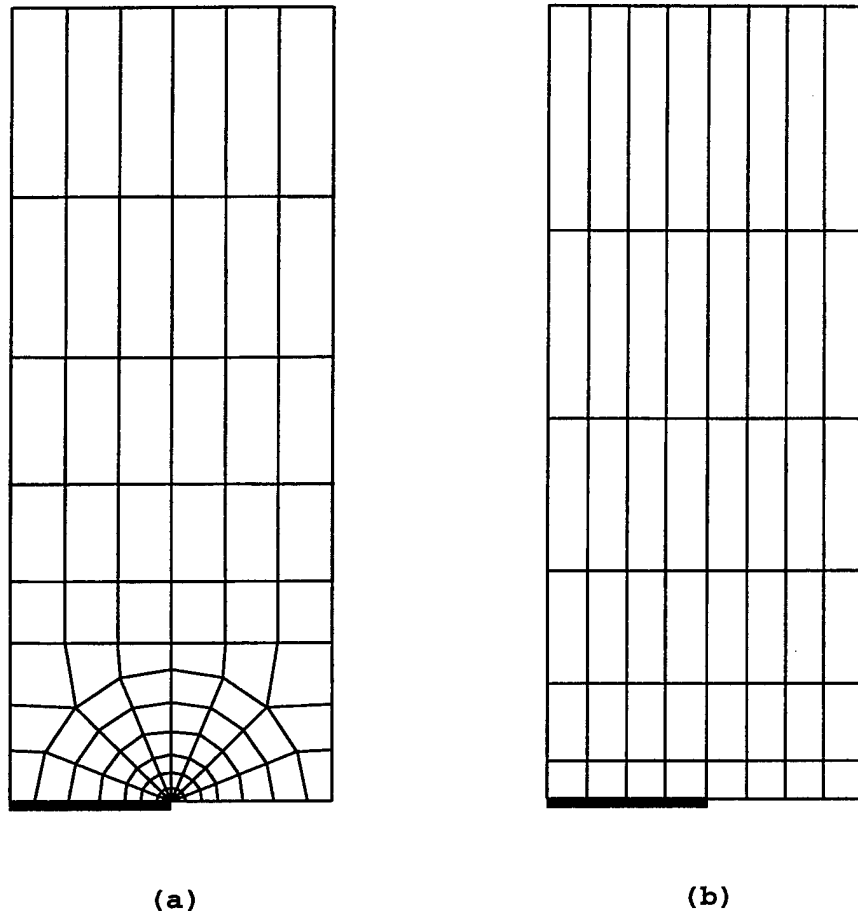


Figure 2.18: The Finite Element Mesh When a) The EDI Method is Used; b) The Finite Element Alternating Method is Used

method. The uncracked body has the same geometry as in the given problem except for the crack. For example, when a crack emanates from a hole in a structure, the hole must still be analyzed in the uncracked structure.

2. Using the finite element solution, the program computes the stresses at the crack location.
3. It then compares the residual stresses calculated in Step 2 with a permissible stress magnitude.
4. The residual stresses at the crack location as computed in Step 2 are reversed to create the traction free crack faces as in the given problem. From this, the program determines a polynomial form for these stresses using a "least squares fit".
5. The analytical solution to the infinite body problem with the crack subject to the polynomial loading calculated in Step 4 is now obtained.

6. The stress intensity factors for the current iteration are then calculated from the analytical solution.
7. The residual stresses on the external surfaces of the body due to the applied loads on the crack faces, are now computed. To satisfy the given traction boundary conditions at the external boundaries, the residual stresses on the external surfaces of the body are reversed and this allows calculation of the equivalent nodal forces.
8. Consider the nodal forces in Step 7 as externally applied loads acting on the uncracked body.

All the steps in the iteration process are repeated until the residual stresses on the crack surface become negligible. It has been observed that this iteration process typically takes three or four steps. The overall stress intensity factor solution is obtained by adding the stress intensity factor solutions for all iterations.

A recent development in the 3D FEAM during Phase II of this project is the development of a numerical scheme for the evaluation of the analytical solution for circular or near circular cracks. The numerical procedure developed by Nishioka and Atluri(1983) becomes numerically unstable as the aspect ratio of the ellipse tends to 1. When the ellipse becomes a circle, this numerical procedure is no longer valid. However, the analytical solution based on the ellipsoidal potential [Vijayakumar and Atluri (1981)] is still valid. An alternative numerical procedure was developed during Phase II of this project. This alternative numerical procedure is documented in this section; while the reader is referred to Vijayakumar and Atluri (1981) and Nishioka and Atluri(1983) for other details on the analytical solution based on the ellipsoidal potentials.

Numerical difficulties arise in the evaluation of the generic elliptical integral  $L_{ijm}$ , defined as

$$L_{ijm} = \int_0^u \text{sn}^{2i} u \text{nd}^{2j} u \text{nc}^{2m} u \, du \quad (2.25)$$

where  $\text{nd} u$ ,  $\text{sn} u$ , and  $\text{nc} u$  are Jacobian elliptical functions.

The numerical procedure introduced by Nishioka and Atluri(1983) uses a recursive formula starting from the evaluation of the integrals

$$I_{nd}^n = \int_0^u \text{nd}^{2n} u \, du \quad n = 0, \pm 1, \pm 2, \dots, \quad (2.26)$$

Let  $a$  be the semi-major axis;  $b$  be the semi-minor axis; and  $k' = b/a$  be the aspect ratio of the ellipse.  $k^2 = 1 - k'^2$ . It is seen that as  $k' \rightarrow 1$ ,  $k \rightarrow 0$ . The recursive formula makes use of the identity  $k^2 \text{sn}^2 u + \text{dn}^2 u = 1$  to evaluate  $\text{sn}^2 u$  for a given  $\text{dn}^2 u$ . However, this formula breaks down when  $k = 0$ , since  $\text{dn}^2 u \equiv 1$  in this case. Alternatively, we can evaluate  $\text{dn}^2 u$  for a given  $\text{sn}^2 u$ . Thus, we can start the recursive formula from the evaluation of the integrals

$$I_{sn}^n = \int_0^u \text{sn}^{2n} u \, du \quad n = 0, 1, 2, \dots, \quad (2.27)$$

Two numerical schemes were developed to evaluate  $I_{sn}^n$  in Phase II of this project. One is for the case where  $k$  is close to 1; and the other is used for small  $k$ .



For small  $k$ , the integral is represented in terms of a series.

$$I_{sn}^n = \int_0^u \text{sn}^{2n} u du = \sum_{i=0}^{\infty} a_i I_{sn}^{n+i} \quad n = 0, 1, 2, \dots, M+2 \quad (2.28)$$

where  $\sin \phi = \text{sn } u$ , and

$$a_i = \frac{2i-1}{2i} k^2 \times a_{i-1} = b_i k^2 a_{i-1}, \quad a_0 = 1 \quad (2.29)$$

and

$$I_{sin}^n = \int_0^\phi \sin^{2n} \phi d\phi.$$

It is evaluated using the following recursive formula.

$$I_{sin}^n = b_n I_{sin}^{n-1} - \frac{c_n}{2n} \quad n = 0, 1, 2, \dots \quad (2.30)$$

where  $I_{sin}^0 = \phi$  and

$$b_n = \frac{2n-1}{2n}, \quad c_n = c_{n-1} \times \sin^2 \phi, \quad c_1 = \sin \phi \cos \phi. \quad (2.31)$$

For large  $k$ , the recursive formula is

$$I_{sn}^{n+1} = \frac{q_n I_{sn}^n + r_n I_{sn}^{n-1} + \alpha_n}{p_n} \quad (2.32)$$

where

$$p_n = (1+2n)k^2, \quad q_n = 2n(1+k^2), \quad r_n = (1-2n). \quad (2.33)$$

$$\alpha_n = \alpha_{n-1} \times \text{sn}^2 u, \quad \alpha_1 = \text{sn } u \text{ cn } u \text{ dn } u \quad (2.34)$$

$$I_{sn}^0 = F(\phi), \quad I_{sn}^1 = \frac{F(\phi) - E(\phi)}{k^2} \quad (2.35)$$

Once  $I_{sn}^n$  are evaluated,  $L_{ijm}$  can be computed using the following scheme. First, compute

$$L_{i,0,0} = I_{sn}^i \quad i = 0, 1, \dots, M \quad (2.36)$$

$$L_{i,-1,0} = I_{sn}^i - k^2 I_{sn}^{i+1} \quad i = 0, 1, \dots, M+1 \quad (2.37)$$

$$L_{i,0,-1} = I_{sn}^i - I_{sn}^{i+1} \quad i = 0, 1, \dots, M \quad (2.38)$$

$$L_{i,-1,-1} = L_{i,-1,0} - L_{i+1,-1,0} \quad i = 0, 1, \dots, M \quad (2.39)$$

Then, compute  $L_{i,j,0}$  and  $L_{i,j,-1}$  for  $j = 0, 1, \dots, (M-1)$

$$L_{i,(j+1),m} = \frac{q_j L_{ijm} + r_j L_{i,(j-1),m} + \alpha_j}{p_j} \quad (2.40)$$

where

$$p_j = (1+2j)k'^2 \quad (2.41)$$

$$q_j = 2[(2j + m - i) + (i - j)k^2] \quad (2.42)$$

$$r_j = 1 + 2(i - j - m) \quad (2.43)$$

$$\alpha_j = \alpha_{j-1} \times \text{nd}^2 u \quad (2.44)$$

$$\alpha_0 = -k^2 \text{sn}^{2i+1} u \text{cn}^{1-2m} u / \text{dn} u \quad (2.45)$$

Here,  $m = 0$  or  $m = -1$ . Therefore, no singular term exists.

Then, compute  $L_{ijm}$  for  $m = 0, 1, \dots, (M - 1 - j)$  using the following recursive formula.

$$L_{i,j,(m+1)} = \frac{q_m L_{ijm} + r_m L_{i,j,(m-1)} + \alpha_m}{p_m} \quad (2.46)$$

where

$$p_m = (1 + 2m)k'^2 \quad (2.47)$$

$$q_m = 2[(i - j - 2m)k^2 + (m - i)] \quad (2.48)$$

$$r_m = [-1 + 2(m + j - i)]k^2 \quad (2.49)$$

$$\alpha_m = \alpha_{m-1} \times \text{nc}^2 u \quad (2.50)$$

$$\alpha_0 = \text{sn}^{2i+1} u \text{nd}^{2j-1} u \text{nc} u \quad (2.51)$$

Singular terms exist as  $\text{cn} u \rightarrow 0$ . In this case,  $\text{sn} u = 1$  and  $\text{dn} = \sqrt{1 - k^2}$

$$\lim_{\text{cn} u \rightarrow 0} \text{cn}^{2m+1} L_{i,j,(m+1)} = \frac{\text{sn}^{2i+1} u \text{nd}^{2j-1} u}{p_m} \quad (2.52)$$

The recursive formula can be derived from the integration of

$$[\text{sn}^{2i+1} u \text{nd}^{2j-1} u \text{nc}^{2m+1} u]'.$$

Note, the following recursive formula is only used for the case where  $j = 0$ ,  $m = 0$  and  $k$  is large enough.

$$L_{(i+1),j,m} = \frac{q_i L_{ijm} + r_i L_{(i-1),j,m} + \alpha_i}{p_i} \quad (2.53)$$

where

$$p_i = [1 + 2(i - j - m)]k^2 \quad (2.54)$$

$$q_i = 2[(i - m) + (i - j)k^2] \quad (2.55)$$

$$r_i = 1 - 2i \quad (2.56)$$

$$\alpha_i = \alpha_{i-1} \times \text{sn}^2 u \quad (2.57)$$

$$\alpha_1 = \text{sn} u \text{nd}^{2j-1} u \text{nc}^{2m-1} u \quad (2.58)$$

One recent application [O'Donoghue, Atluri and Pipkins (1995)] of the FEAM was to the analysis of fatigue cracking in the lower wing skin of the U.S. Air Force C-141B (Fig. 2.19). In this application, the growth of corner cracks from the weep holes located in the integral risers of



Figure 2.19: U.S. Air Force C-141B

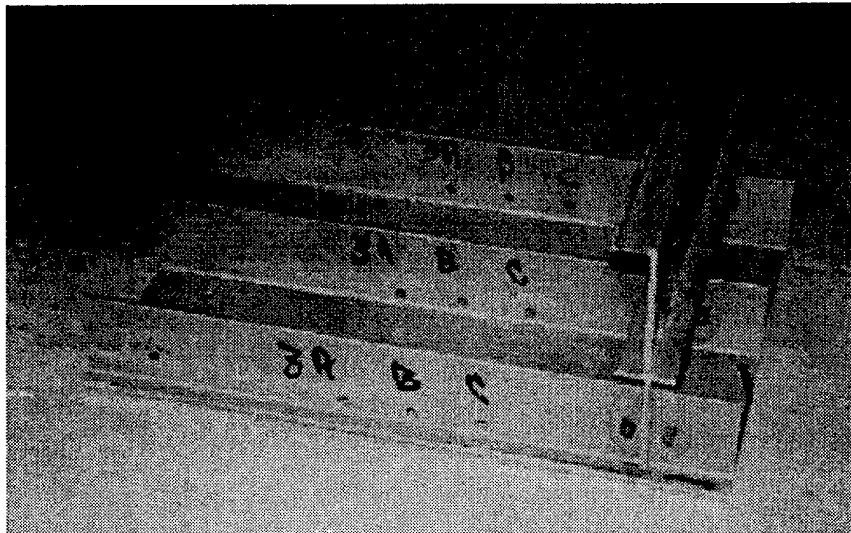


Figure 2.20: Cut-Out Lower Wing Panel from the C-141B Showing Weep Holes

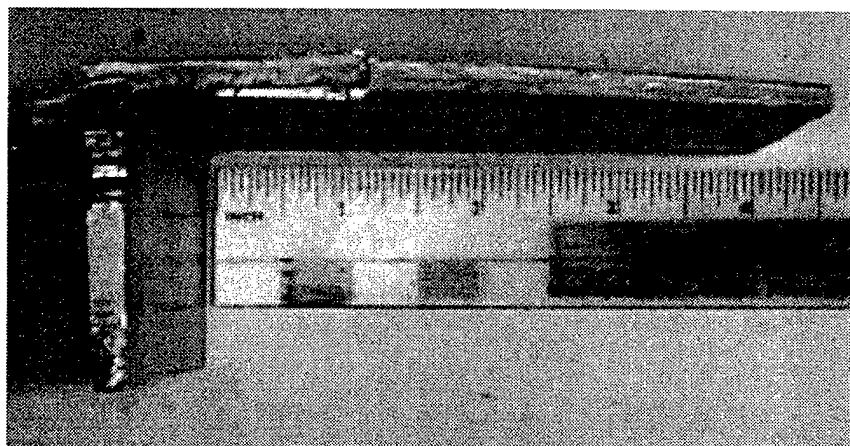


Figure 2.21: Cross-Section of Failed Lower Wing Panel of the C-141B

the wing skin was modeled with the FEAM (Fig. 2.20 and Fig. 2.21). Fatigue crack growth predictions were made wherein the FEAM was used to generate stress intensity factors which were in turn used in a Forman equation. The load spectrum used was comprised of peak-valley pairs representing 3027 equivalent flight hours. Comparisons with limited test data showed good correlation between the FEAM based fatigue crack growth predictions and the experimental data.

#### ***2.5.6 Distributed-Dislocation-base FEAM for curved cracks***

A curved crack can be treated as a distribution of dislocations. To construct the analytical solution for a curved crack in an infinite sheet, one can solve for the dislocation density for the curved crack. Using a complex stress function approach, the dislocation density can be related to the crack surface traction [Park and Atluri(1998), Chen(1993), and Cheung and Chen(1987)]. Once the dislocation density is solved for, the stress and displacement in the infinite sheet, subjected to the prescribed crack surface traction, can be obtained.

The formulation in Park and Atluri(1998) is used for the construction of the dislocation-based analytical solutions for a curved crack, subjected to arbitrary crack surface tractions. Using these solutions with the finite element solution for a sheet of finite size, a Dislocation-based FEAM is implemented for the curved cracks in a finite sheet.

### **2.6 Fatigue crack growth**

#### ***Fatigue Crack Growth***

The problem of fatigue crack growth is of considerable practical importance when designing a structure which satisfies the DTR. To successfully employ damage tolerance principles, an accurate determination is required of the number of load cycles to failure in a component. These estimates

will have a significant influence in the design and maintenance of a safe structure such as in the scheduling of inspection intervals.

Fatigue crack growth frequently occurs when a flawed component is subject to some form of cyclic loading. Here the crack growth is termed subcritical since, due to the cyclic loading, it takes place at stress intensity factor levels that are less than the fracture toughness of the material. The form of the cyclic loading is also of great importance such as whether it has constant amplitude or has a variable amplitude. The damage tolerance module has the capability to model fatigue crack under conditions of constant amplitude and variable amplitude loading. This capability is limited to self similar (i.e. Mode I) crack growth.

The crack growth calculations will be performed based on stress intensity factors obtained either by the FEAM or user supplied beta factors. For reasons of computational efficiency and accuracy, the user can use the FEAM to update the beta factor after the crack growth exceeds a specific amount. Fatigue crack growth is carried out using the beta factor, assuming that a small amount of crack growth does not effect the beta factor. When the amount of crack growth exceeds the threshold specified by the user, the FEAM can be invoked to update the beta factor.

The FEAM has made the use of finite elements in fatigue calculations feasible. The reason being that the global stiffness matrix of the finite element model is assembled and decomposed only once, since the stiffness of the uncracked structure remains the same for all crack sizes. In other finite element approaches, such as those using singular/hybrid type special crack-tip finite elements or using EDI methods, the cracks must be modeled explicitly. Therefore, the global stiffness matrix must be assembled and decomposed for each crack size. The assembly and decomposition of the global stiffness matrix accounts for about 80% of the computational time required in a typical finite element analysis. Given that the FEAM has to perform this operation only once during a fatigue analysis, the benefits of this approach over other finite element techniques for fatigue crack growth are readily apparent.

Load spectra, in terms of ASTROS' load cases, is provided to the damage tolerance module by the USAGE module described in Nees (1995). Since the USAGE module defines aircraft maneuvers in terms of ASTROS load cases, the load spectra at any point in the aircraft structure is automatically determined by extracting stresses at that point from the ASTROS solution database. Use is made of USAGE features such as repeating and blocking of data to minimize storage and/or computational requirements of variable amplitude crack growth calculations.

Numerous studies have been conducted on the characteristics of fatigue crack growth. It has been established that when the plastic or inelastic zone in the vicinity of the crack is small, then the stress intensity factor is the governing parameter during crack growth [Paris and Erdogan (1963)]. In general, the crack growth rate is a function of stress intensity factor change, which is given by:

$$\Delta K = K_{max} - K_{min} \quad (2.59)$$

where  $K_{max}$  is the maximum stress intensity factor during the load cycle and  $K_{min}$  is the minimum value of the stress intensity factor. Based on the minimum and maximum loads, it is customary to define the parameter  $R$  where:

$$R = K_{min}/K_{max} \quad (2.60)$$

An important point must be made in relation to the functional relationship between the fatigue crack growth rate and the change in stress intensity factor. This crack growth rate function can be partitioned into three separate regions. At low values of  $\Delta K$ , there is very little crack growth with a negligible crack growth rate. Therefore, it can be stated that there exists a  $\Delta K$  below which there is no crack growth. This quantity is referred to as the threshold stress intensity factor and is denoted as  $(\Delta K)_{th}$ . At higher values of  $\Delta K$ , crack growth takes place. It has been observed experimentally that this curve, relating the crack growth rate,  $da/dN$ , to  $\Delta K$ , is usually linear on a log-log plot and this corresponds to a power law relation between  $da/dN$  and  $\Delta K$ . This is commonly referred to as the Paris relation and is given as [Paris, Gomez and Anderson (1961)]:

$$\frac{da}{dN} = C(\Delta K)^n \quad (2.61)$$

where  $a$  is the crack length and  $N$  is the number of load cycles. The quantities  $C$  and  $n$  are material dependent constants. At higher values of  $\Delta K$  the stress intensity factor is approaching the fracture toughness of the material,  $K_c$ . The crack growth rate will increase significantly, eventually leading to the onset of rapid unstable crack growth.

Recognizing that several distinct phases in fatigue crack growth exist, a more general form for the relationship between crack growth rate and stress intensity factor is expressed as:

$$\frac{da}{dN} = \frac{C(1-R)^m(\Delta K)^n\{\Delta K - (\Delta K)_{th}\}^p}{\{(1-R)K_c - \Delta K\}^q} \quad (2.62)$$

where  $m$ ,  $p$  and  $q$  are constants that relate to the particular crack growth relation that is being used. By assigning different values to these quantities some of the well known crack growth relations can be recovered. For example, when  $m = p = q = 0$ , the Paris relation is obtained. The Forman relation [Forman, Kearney and Engle (1967)], which accounts for high crack growth rates and instability, is recovered by setting  $m = p = 0$  and  $q = 1$ . By setting  $p = q = 0$  and  $m = (M_w - 1)n$ , the Walker relation [Walker (1970)] is derived, where  $M_w$  is an exponent in the Walker relation.

With stress intensity factor solutions and a crack growth relation in hand, the ultimate objective of fatigue crack growth calculations, to calculate the number of cycles for a crack to grow by a specified amount, can be carried out. This is done by integrating the growth relation [Equation (2.61) or (2.62)]. For example, the equation (2.61) is integrated as follows. Since

$$\Delta K = \Delta \sigma \sqrt{\pi a}$$

Eq. 2.61 can be rewritten as

$$\frac{da}{dN} = C_1 a^{n/2}$$

where  $C_1 = C [\beta \Delta \sqrt{\pi}]^n$ . Assuming that the beta factor does not change for the small amount of crack growth in  $N$  cycles, the amount of crack growth is

$$\Delta a = a_o \left[ 1 + (1 - n/2) \frac{CN(\Delta K)^n}{a_o} \right]^{1/(1-n/2)} - a_o \quad \text{for } n \neq 2$$

or

$$\Delta a = a_o e^{\left[ \frac{CN(\Delta K)^n}{a_o} \right]} - a_o \quad \text{for } n = 2$$

where  $a_o$  is the half crack length before the  $N$  cycles crack growth. The integration is carried out for a specific design life to find the final crack length at the end of the design life of the aircraft. All of these steps will be carried out automatically by the damage tolerance module.

Self-similar growth of through skin cracks is straightforward to carry out using the above procedure. However, for an elliptical or part elliptical crack since the stress intensity factor distribution is generally not constant along the elliptical crack front, the crack growth rates will not be the same in every direction. Consequently, the shape of the crack will change. It has been often observed in practice that a semi-elliptical surface crack, initially having a small aspect ratio, will have a larger crack growth rate in the minor axis direction. The damage tolerance module computes the amount of crack growth for the major and minor axis, assuming that the orientation of the major/minor axis does not change. The situation where the minor axis grows faster than the major axis so that it becomes the major axis after a numbers of cycles is allowed by the damage tolerance module.

## 2.7 Optimization

The principal objective of multi-disciplinary structural optimization is to minimize an objective function such as structural weight and/or cost subject to discipline specific constraints (strength, flutter, stiffness, etc.). ASTROS provides a sophisticated software framework for performing such optimizations. ASTROS supports both preliminary design and design modifications that occur later in the product life cycle. It combines finite element modeling and analysis techniques with efficient optimization algorithms to deliver significant reductions in the time required to develop superior designs of structures. The finite element modeling is based on the standard NASTRAN bulk data format.

The preliminary design stage is where ASTROS capabilities can be used to the fullest. Typically, the aerodynamic configuration, materials and design conditions have been defined at this stage. The preliminary design challenge is then to determine the optimal (i.e. least weight and/or cost) structural configuration which satisfies constraints imposed by multiple engineering disciplines. ASTROS supports a wide variety of constraints. These include: Tsai-Wu stress criteria; von-Mises stress; stiffness; natural frequency; flutter; laminate composition; panel and beam buckling; and aeroelastic lift and control effectiveness. With the addition of the damage tolerance module, residual strength and residual life based constraints are now part of this list. ASTROS performs the optimization task by automatically changing design variables. The design variables which ASTROS uses are related to properties of the finite elements used to model the structure being optimized. The design variables are the thickness of shell elements and cross-sectional area of beam elements. For laminates, the thickness of individual plies is the design variable. In order to insure that the optimized structure is realistic from a manufacturing point of view ASTROS supports design variable linking. Design variable linking allows the grouping of elements for constant thickness structure or the definition of shape functions for tapered (thickness) structure.

The damage tolerance module evaluates the residual strength and residual life based constraints based on damage tolerance analysis. However, automated redesign based on the damage tolerance constraint is still not well resolved. Based on the factor that damage tolerance analysis takes a significant amount of time, while the damage tolerance constraint is not the most important constraint during the preliminary design, it is suggested that the user used beta-factor based automated redesign strategy. The details follow. The user can use the damage tolerance module to evaluate the beta factors as correction factors for an analytical solution for a simple case. The constraint can then be expressed explicitly in using a formula involving the beta factor. This constraint can be defined by the user in terms of a user defined function in ASTROS. Assuming that the beta factor does not change during the redesign, one can use the existing capability of ASTROS to perform automated redesign. After the redesign, the beta factor can be re-evaluated to ensure that the damage tolerance constraint is met. This approach can significantly reduce the computational time associated with the computation of damage tolerance constraints.

## 2.8 Interfacing with ASTROS

This section briefly summaries the interfacing techniques used to integrate the damage tolerance module with **ASTROS** (**A**utomated **S**TRuctural **O**ptimization **S**ystem). More details can be found in the *Interface Design Document* for this project.

ASTROS is an extendible system built on top of an engineering database and the **Matrix Analysis Problem Oriented Language** (MAPOL). The database provides a channel for the inter-module communication in ASTROS; while MAPOL provides extendibility to ASTROS. During the integration of the damage tolerance module into ASTROS, an extremely powerful “gluing tool” – **Tool Command Language** (TCL) is introduced into ASTROS.

The damage tolerance module is a complex system by itself. It includes customized mesh generators, finite element alternating [Schwartz-Neumann Alternating] codes (for 2D straight cracks, 2D curved cracks and 3D elliptical/circular cracks), an automated Global/Local analyzer, and a buckling analyzer. They were developed using different computer languages, such as C, C++ and FORTRAN. In order to integrate the damage tolerance module into ASTROS, a TCL interpreter is planted into ASTROS as a module invokable from a MAPOL sequence.

Fig. 2.22 shows the interfacing strategy for incorporating damage tolerance into ASTROS. It is seen in Fig. 2.22 that the Damage Tolerance Module communicates with the other Built-in Modules of ASTROS through the Engineering Database. The extended modules are controlled by TCL scripts, which are interpreted by the embedded TCL interpreter. The interpreter is in turn controlled by the modified MAPOL sequence.

Interfacing aspects, related to MAPOL, DATABASE and TCL, are documented in this chapter. Database entities used by the damage tolerance module to communicate with other modules are described in the *Interface Design Document*.



### 2.8.1 MAPOL

As seen in Fig. 2.22, the MAPOL sequence does not control the damage tolerance module directly. It interacts with the TCL module only.

A single argument (INTEGER) is passed to the TCL module from the MAPOL calling sequence. This argument indicates the position in the MAPOL sequence, from which the MAPOL call is placed. This status indicator is set as the value of the global TCL variable `astrosStateID`. Depending on the value of `astrosStateID`, the TCL module i) creates an interpreter; ii) performs input data check; iii) performs damage tolerance analysis; or iv) deletes the interpreter, etc. No other direct data communication is made between the MAPOL calling sequence and the damage tolerance module. The damage tolerance module communicates with the rest of the modules in ASTROS, through the database entities, to get the data required for damage tolerance analyses. It also stores the results in the database for other modules to access.

### 2.8.2 DATABASE

ASTROS relies on the engineering database for inter-module communication. Originally based on the Computer Automated Design Database (CADDDB), which was the heart of ASTROS during its development, the commercially supported ASTROS is now based on the eBASE database developed by UAI. In this project, the set of interface routines for CADDDB are used to access database entries. To facilitate the migration from CADDDB to eBASE, the damage tolerance module uses a set of TCL commands to access the database via the CADDDB interface. To migrate from the CADDDB interface to the eBASE interface, it will be necessary to re-implement only those TCL commands using the eBASE access routines.

### 2.8.3 TCL

Tool Command Language (TCL) is a simple, yet robust scripting language. It is an excellent scripting language for extending the functionality of existing programs. TCL was originally developed at the University of California, Berkeley. The development was later shifted to Sun Microsystems, Inc. Currently, it is commercially supported by Scriptics, Inc. The core system of TCL is freely distributed with the source code. Although it is distributed without a charge, it is very stable and of commercial quality. TCL has become an increasingly popular cross-platform scripting language. Many commercial software have been developed based on TCL.

TCL consists of a scripting language and an interpreter for that language. TCL interpreter is designed such that it can be easily embedded into other applications. As a language, it is much like the UNIX shell language. There is very little syntax; and it is very easy to learn. TCL has been used to assemble software modules that have been built in system programming languages like C, C++ and FORTRAN. These building blocks appear as commands, or verbs, in TCL.

Online user manuals are available at Scriptics' web site (<http://www.scriptics.com/man/tcl8.0/contents.htm>). Much more helpful information can be found at <http://www.scriptics.com/resource/>.

The damage tolerance module is actually a complex system. It includes customized mesh generators, finite element alternating codes [based on the Schwartz-Neumann alternating method](for 2D straight cracks, 2D curved cracks and 3D elliptical/circular cracks), an automated Global/Local analyzer, and a buckling analyzer. They were developed using different computer languages, such as C, C++ and FORTRAN. In order to integrate the damage tolerance module into ASTROS, a TCL interpreter was planted into ASTROS as a module invocable from the MAPOL sequence.

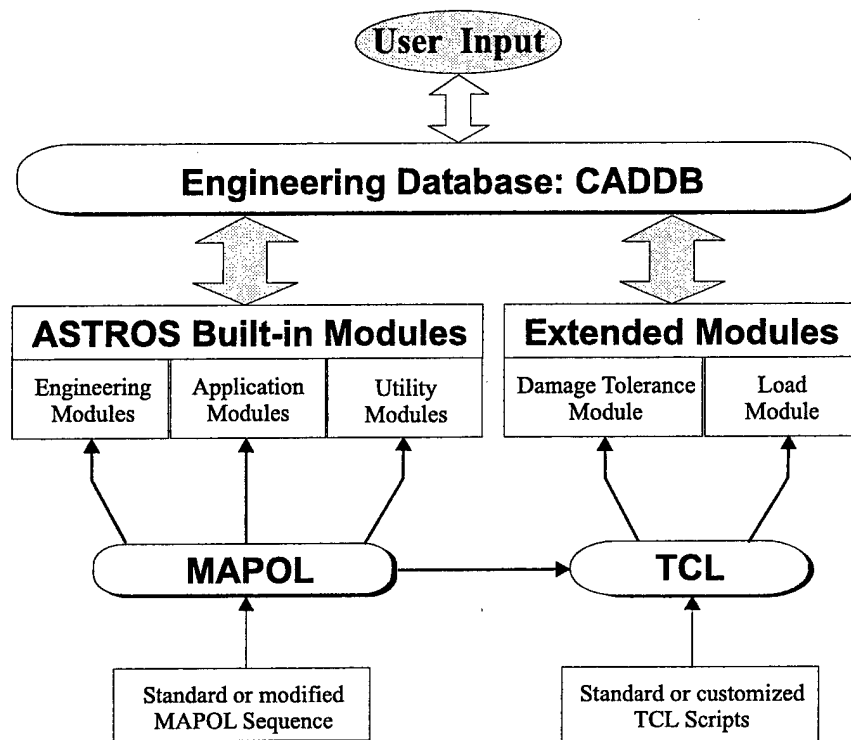


Figure 2.22: Integration of damage tolerance module with ASTROS

## **CHAPTER III**

### **SUMMARY OF PHASE II ACCOMPLISHMENTS**

A summary of the Phase II accomplishments in this SBIR project is presented in this chapter.

During Phase II, a damage tolerance module is implemented and integrated with ASTROS. To integrate the damage tolerance module into ASTROS, the TCL (Tool Command Language) interpreter has been implanted into ASTROS as a gluing tool.

Customized damage tolerance models have been implemented so that the user can easily perform these types of damage tolerance analysis with very little effort. A master element approach has been used to minimize the impact of damage tolerance analysis on the data preparation for the preliminary design model. With a few extra bulk data cards, the user can perform damage tolerance analysis.

The customized damage tolerance models that have been implemented are:

- Discrete Source Damage Model: a lead crack in a stiffened panel with/without the presence of a broken central stiffener [Fig. 2.7]
- BuckDel Model: buckling of a composite panel in the presence of a delamination [Fig. 2.8]
- Straight Crack Model: a panel with a centered crack [Fig. 2.1]
- Rivet Hole Crack model: one (or two) crack(s) emanating from one side (or both sides) of a rivet hole [Fig. 2.2]
- Curved Crack model: a panel with a curved crack [Fig. 2.5]
- Rivet Hole Curved Crack model: one (or two) curved crack(s) emanating from one side (or both sides) of a rivet hole [Fig. 2.6]
- Surface crack model: one centered surface crack in a plate [Fig. 2.3]
- Rivet Hole Corner Crack model: two corner cracks emanating from both side of a straight-shank rivet hole. [Fig. 2.4]

An automated global-local analyzer was developed for the analysis of discrete source damage. The automated global-local analyzer, based on the feature modeling technique, has an integrated geometry modeler and mesh generator. It completely automates the model simplification, model generation and submodel creation for a hierarchical analysis.

A 2D FEAM (Finite element alternating method), 3D FEAM, and distributed dislocation based FEAM have been implemented in the damage tolerance module for the analyses of 2D straight cracks, 3D surface flaws/corner crack, and 2D curved cracks. An alternative numerical scheme has been developed to overcome the difficulties associated with the cracks of a circular shape.

The damage tolerance module can generate a cyclic loading spectrum, based on the user defined loading spectrum (in terms of ASTROS loading cases). Using this cyclic loading spectrum, the damage tolerance module can perform self-similar (Mode I) fatigue crack growth analysis.

The damage tolerance module was integrated into ASTROS v20p0 on AIX 4.2. It has been ported on the IRIX operating system.

## REFERENCES

- [1] Atluri, S.N. (1986) : *Computational Methods in the Mechanics of Fracture*. Amsterdam: North Holland, also translated into Russian, Mir Publishers, Moscow(1989).
- [2] Atluri, S. N. (1995) : *Failure Processes in, and Integrity of, Composite Structures; & Life Enhancement of Aging Aircraft*, ICCE/2, Second International Conference on Composite Engineering, Edited by David Hui, August 21-24, 1995, New Orleans, pp. A47-A50.
- [3] Atluri, S.N., et. al. (1992): *Composite Repairs of Cracked Metallic Aircraft Structures*, DOT Report No. DOT/FAA/CT-92/32, June 1992.
- [4] Britt, V.O. (1994):*Shear and Compression Buckling Analysis for Anisotropic Panels with Elliptical Cutouts* AIAA Journal, Vol. 32, No. 11. pp.551-574.
- [5] Brust, F.W.; Atluri, S.N. (1986):*Studies on creep crack growth using the  $T^*$  integral*. Engineering Fracture Mechanics, Vol.23, No.3. pp. 2293-2299.
- [6] Chen, Y.Z. (1993):*Numerical solution of a curved crack problem by using hypersingular integral equation approach* Eng. Frac. Mech. v 46 pp.275-283
- [7] Cheung, Y.K.; Chen Y.Z. (1987):*New integral equation for plane elasticity crack problems*. Theoretical and Applied Fracture Mechanics, v 7, pp.177-184
- [8] Forman, R.G., Kearney, V.E., Engle, R.M. (1967): *Numerical Analysis of Crack Propagation in Cyclic-Loaded Structures*, Journal of Basic Engineering, v 89, pp. 459-464.
- [9] Huang, B-Z.; Atluri, S. N. (1995) : *A simple method to follow post-buckling paths in finite element analysis*. Computers and Structures, v 57, n 3, 477-489
- [10] Muskhelishvili, N.I. (1953) : *Some Basic Problems of the Mathematical Theory of Elasticity*. Noordhoo, Groningen.
- [11] Nees, C.D. (1995): *Methodology for Implementing Fracture Mechanics in Global Structural Design of Aircraft*, Masters Thesis, Air Force Institute of Technology, Wright-Patterson AFB, OH.
- [12] Nemeth, M.P. (1990) : *Buckling and Postbuckling Behavior of Compression-Loaded Isotropic Plates with Cutouts*, AIAA Publication No. AIAA-90-0965-CP, pp. 862-876.
- [13] Nishioka, T.; Atluri, S.N. (1980) : *Assumed stress finite element analysis of through-cracks in angle-ply laminates*. AIAA Journal v 18 n 9 1980 p 1125-1132
- [14] Nishioka, T.; Atluri, S.N. (1983) : *Analytical solution for embedded elliptical cracks, and finite element alternating method for elliptical surface cracks, subjected to arbitrary loadings*. Eng Fract Mech, v 17 n 3, 1983, p 247-268.
- [15] O' Donoghue, P. E.; Nishioka, T.; Atluri, S. N. (1984) : *Multiple surface cracks in pressure vessels*. Eng Fract Mech v 20 n 3 1984 p 545-560

- [16] O'Donoghue, P. E.; Nishioka, T.; Atluri, S. N. (1985) : *Multiple coplanar embedded elliptical cracks in an infinite solid subject to arbitrary crack face tractions*. Int J Numer Methods Eng v 21 n 3 Mar 1985 p 437-449
- [17] O'Donoghue, P.E.; Atluri, S.N.; Pipkins, D.S. (1995) : *Computational strategies for fatigue crack growth in three dimensions with application to aircraft components*. Eng Fract Mech 52 1 Sept 1995 Pergamon Press Inc Tarrytown NY USA p 51-64
- [18] Paris, P.C., Erdogan, F. (1963): *A Critical Analysis of Crack Propagation Laws*, Journal of Basic Engineering, v 85, pp. 528-534
- [19] Paris, P.C., Gomez M.P., Anderson W.E. (1961): *A Rational Analytic Theory of Fatigue*, The Trend in Engineering, v 13, pp. 9-14
- [20] Park, J.H.; Atluri, S.N. (1993) : *Fatigue growth of multiple-cracks near a row of fastener-holes in a fuselage lap-joint*. Computational Mechanics v 13 n 3 Dec 1993. p 189-203.
- [21] Park, J.H.; Atluri, S.N. (1998) : *Mixed mode fatigue growth of curved cracks emanating from faster holes in aircraft lap joints* Computational Mechanics v 21 p 477-482.
- [22] Pipkins, D.S.; Atluri, S.N. (1996) : *BUCKDEL v0.9 Users and Theory Manuals* Wright Laboratory Technical Report No. WL-TR-96-xxx.
- [23] Vellaichamy, S., Prakash, B.G., and Brun, S. (1990) : *Optimum Design of Cutouts in Laminated Composite Structures*, Computers & Structures, Vol. 37 No. 3, pp. 241-246.
- [24] Vijayakumar, K.; Atluri, S.N. (1981) : *An embedded elliptical crack, in an infinite solid, subjected to arbitrary crack-face tractions*. J Appl Mech Trans ASME v 103 n 1 Mar 1981 p 88-96
- [25] Walker, K. (1970): *The Effect of Stress Ratio During Crack Propagation and Fatigue for 2024-T3 and 7075-T6 Aluminum*, in Effects of Environment and Complex Load History on Fatigue Life, ASTM STP 462, published by the American Society for Testing and Materials, pp. 1-14.
- [26] Wang, L.H.; Atluri, S.N. (1995) : *Implementation of the Schwartz-Neumann alternating method for collinear multiple cracks with mixed type of boundary conditions*. Comput Mech v 16 n 4 p 266-271
- [27] Wang, L.H.; Atluri, S.N. (1996) : *Recent advances in the alternating method for elastic and inelastic fracture analyses*. Computer Methods in Applied Mechanics & Engineering, 137(1), 1-58.
- [28] Wang, L.H.; Brust, F.W.; Atluri, S.N. (1995a) : *The elastic-plastic finite element alternating method (EPFEAM) and the prediction of fracture under WFD conditions in aircraft structures. Part I. EPFEAM theory*. FAA Center of Excellence Report, August, 1995.
- [29] Wang, L.H.; Brust, F.W.; Atluri, S.N. (1995b) : *The elastic-plastic finite element alternating method (EPFEAM) and the prediction of fracture under WFD conditions in aircraft structures. Part II. Fracture and the  $T^*$ -integral parameter*. FAA Center of Excellence Report, August, 1995.
- [30] Wang, L.H.; Brust, F.W.; Atluri, S.N. (1995c) : *The elastic-plastic finite element alternating method (EPFEAM) and the prediction of fracture under WFD conditions in aircraft structures. Part III. Computational Predictions of the NIST multiple site damage experimental results*. FAA Center of Excellence Report, August, 1995.